

# CoGenCast: A Coupled Autoregressive–Flow Generative Framework for Time Series Forecasting

Yaguo Liu<sup>1</sup> Mingyue Cheng<sup>1</sup> Daoyu Wang<sup>1</sup> Xiaoyu Tao<sup>1</sup> Qi Liu<sup>1</sup>

## Abstract

Time series forecasting can be viewed as a generative problem that requires both semantic understanding over contextual conditions and stochastic modeling of continuous temporal dynamics. Existing approaches typically rely on either autoregressive large language models (LLMs) for semantic context modeling or diffusion-like models for continuous probabilistic generation. However, neither method alone can adequately model both aspects simultaneously. In this work, we propose CoGenCast, a hybrid generative framework that couples pre-trained LLMs with flow-matching mechanism for effective time series forecasting. Specifically, we reconfigure pre-trained decoder-only LLMs into a native forecasting encoder–decoder backbone by modifying only the attention topology, enabling bidirectional context encoding and causal representation generation. Building on this, a flow-matching mechanism is further integrated to model temporal evolution, capturing continuous stochastic dynamics conditioned on the autoregressively generated representation. Notably, CoGenCast naturally supports multimodal forecasting and cross-domain unified training. Extensive experiments on multiple benchmarks show that CoGenCast consistently outperforms previous compared baselines. Code is available at [https://github.com/liuyaguo/\\_CoGenCast](https://github.com/liuyaguo/_CoGenCast).

## 1. Introduction

Time series forecasting supports a wide range of real-world decision-making processes, including energy (Zhou et al., 2024), finance (Feng et al., 2019) and healthcare (Cheng et al., 2024). The core philosophy of forecasting (Liu et al., 2023) is to predict future values conditioned on historical

<sup>1</sup> State Key Laboratory of Cognitive Intelligence, University of Science and Technology of China, Hefei, China. Correspondence to: Mingyue Cheng <mycheng@ustc.edu.cn>.

Preprint. February 4, 2026.

observations, while future evolution is often full of complexity and uncertainty. To handle this, previous works typically implement a simple regression mapping (Nie et al., 2022). However, recently, an increasing number of methods employ more powerful mapping functions, such as LLMs (Niu et al., 2025; Jiang et al.) and diffusion-like (Guo et al., 2025) models. These methods reformulate forecasting as a conditional generative problem (Wu et al., 2025; Liu et al., 2024c).

Current generative forecasting methods can be divided into two main categories: LLM-based methods and diffusion-like models. First, LLM-based methods leverage the strong semantic understanding and generation capabilities of LLMs. These can be further branched into tuning-based methods (Jin et al., 2023; Xie et al., 2024), which finetune LLMs to align them with numerical time series modeling, and training-free methods (Liu et al., 2024b; Cheng et al., 2025c), which keep LLMs frozen and rely on prompting or reasoning mechanisms to perform forecasting. Second, diffusion-like models focus on modeling the probabilistic evolution of future time series in continuous-valued spaces. These approaches effectively capture uncertainty in future temporal trajectories. Representative works such as NsDiff (Ye et al., 2025) and TSFlow (Kolloviev et al., 2024) learn continuous stochastic temporal dynamics, enabling high-quality probabilistic generation (Tashiro et al., 2021).

Although the above generative forecasting methods achieve promising results, we argue that an ideal forecasting approach should simultaneously possess dual capabilities: semantic understanding over contextual conditions and stochastic modeling of continuous temporal dynamics. Taking electricity load forecasting (Wang et al., 2024) as a concrete example, a model should achieve a deep understanding of diverse contextual conditions, such as historical load patterns, urban population, and weather variables, to capture the underlying semantic dependencies. Meanwhile, future electricity demand is closely linked to unpredictable future weather shifts, holiday effects, and other uncertain factors (Rasul et al., 2021; Zhang et al., 2024b) requiring stochastic modeling of continuous temporal dynamics.

Building upon the analysis above, we propose CoGenCast, a hybrid generative framework that couples pre-trained LLMs with flow-matching mechanism for effective time series

forecasting. Specifically, we introduce a reconfiguration of pre-trained decoder-only LLMs into a native forecasting encoder-decoder backbone. Instead of retraining LLMs from scratch, we modify only the attention topology to construct a bidirectional encoder for comprehensive understanding over contextual conditions and a causal decoder for autoregressive representation generation. A flow-matching denoising decoder is further integrated to model temporal evolution, effectively capturing continuous stochastic dynamics conditioned on the autoregressively generated representation. Notably, unlike conventional flow-matching methods, our approach targets the mean velocity field, enabling efficient one-step generation with low latency. As a result, CoGenCast naturally supports multimodal forecasting and cross-domain unified training. CoGenCast outperforms previous compared baselines across multiple real-world benchmarks.

We summarize our main contributions as follows:

- We highlight that an ideal forecasting approach should possess dual capabilities: semantic understanding over contextual conditions and stochastic modeling of continuous temporal dynamics.
- We propose CoGenCast, a hybrid generative framework that couples pre-trained LLMs with continuous flow-matching mechanism for time series forecasting.
- We conduct extensive experiments on multiple benchmarks, demonstrating that CoGenCast consistently outperforms previous compared baselines.

## 2. Related Work

### 2.1. LLM-based Time Series Forecasting

Recently, LLM-based (Jin et al., 2024) methods become increasingly prevalent in time series forecasting due to the strong semantic understanding (Pan et al., 2024) and generation (Bian et al., 2024) capabilities of LLMs. Existing LLM-based time series forecasting methods can be broadly categorized into tuning-based and training-free methods. Within the tuning-based category, PromptCast (Xue & Salim, 2023) reformulates forecasting as a sentence-to-sentence task using text prompts; Time-LLM (Jin et al., 2023) utilizes a learnable interface to reprogram continuous patches into the linguistic space; LLM4TS (Chang et al., 2025) combines the LLM’s feature extraction capabilities with a specialized linear head for numerical output; TokenCast (Tao et al., 2025) implements symbolic discretization to map series into a unified vocabulary for autoregressive generation; ChatTS (Xie et al., 2024) aligns time series as a standalone modality with LLMs via synthetic data to enable open-ended reasoning; and Time-R1 (Luo et al., 2025) feeds the entire sequence as a direct reasoning input while employing reinforcement learning to optimize explicit slow-thinking chains. Conversely,

within the training-free category, LLMTIME (Gruver et al., 2023) demonstrates the potential of pre-trained models to extrapolate numerical strings without further training, and TimeReasoner (Cheng et al., 2025c) induces multi-step temporal reasoning via multi-step prompting.

### 2.2. Diffusion-like Time Series Forecasting

Diffusion models become superior generative tools for time series forecasting due to their powerful capabilities of effectively capturing temporal uncertainty. Early research primarily focused on foundational architectural adaptations: TimeGrad (Rasul et al., 2021) pioneers the integration of an autoregressive framework with denoising diffusion models, while CSDD (Tashiro et al., 2021) utilizes a non-autoregressive score-based model to capture spatio-temporal correlations. Subsequent studies shift toward condition-enhanced mechanisms to improve effectiveness: TimeDiff (Shen & Kwok, 2023) introduces future mixup and autoregressive initialization to strengthen pattern capture; NsDiff (Ye et al., 2025) incorporates a location-scale noise model for adaptive noise scheduling in non-stationary data; and DyDiff (Guo et al., 2025) improves forecasting performance by modeling temporal transitions within the diffusion process. To bridge the efficiency gap of iterative diffusion models, flow-matching models has emerged as its faster generation. FlowTS (Hu et al., 2024) accelerates generation by learning straight-line transport paths via rectified flow, while TSFlow (Kolloviev et al., 2024) incorporates Gaussian process priors to align these trajectories with temporal dynamics. Additionally, FreqFlow (Moghadas et al., 2025) shifts the process into the frequency domain to capture long-term patterns. Despite these methods make significant progress, no single approach adequately satisfies the dual requirements of semantic understanding and continuous stochastic modeling. To address this, we propose CoGenCast, a hybrid generative framework that couples pre-trained LLMs with continuous flow-matching mechanism for time series forecasting to model both aspects simultaneously.

## 3. Methodology

In this section, we provide the formal problem definition and present an overview of our proposed CoGenCast. We also detail the implementation process.

### 3.1. Problem Formulation

We consider the time series forecasting problem where the goal is to forecast future sequences based on historical context features and numerical sequences (Cheng et al., 2025b). Let  $\mathbf{X}_{\text{hist}} = \{x_1, \dots, x_L\} \in \mathbb{R}^{L \times D}$  denote the look-back window of length  $L$  with  $D$  variables. The objective is to forecast the predicted window  $\mathbf{X}_{\text{pred}} = \{x_{L+1}, \dots, x_{L+H}\} \in \mathbb{R}^{H \times D}$  of length  $H$ . Additionally,

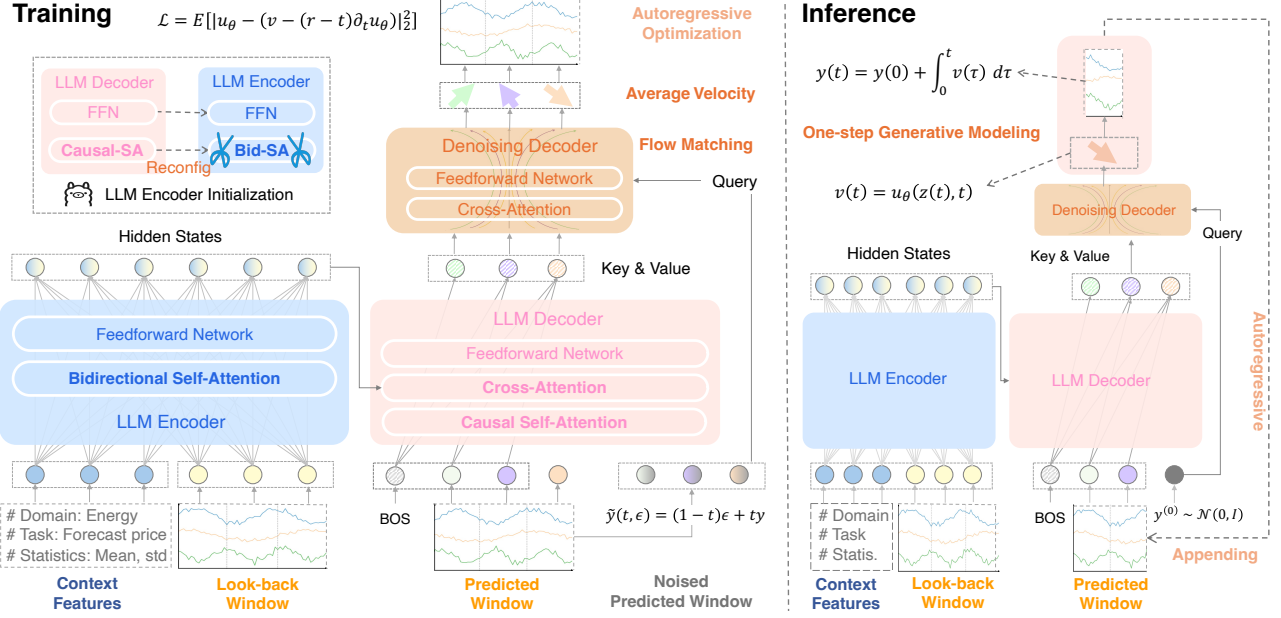


Figure 1. Overview of our proposed CoGenCast. **Left (Training):** We reconfigure decoder-only LLMs into an encoder–decoder backbone by attention-only modification, and perform continuous flow-matching mechanism conditioned on the LLM-generated representation. **Right (Inference):** Future patches are generated autoregressively and sampled via one-step flow-matching generation with low-latency.

let  $\mathbf{C}$  denote the context features (e.g., domain knowledge, task instruction, statistics information). The problem (Cheng et al., 2025a) is formulated as learning the conditional probability distribution  $P(\mathbf{X}_{\text{pred}} | \mathbf{X}_{\text{hist}}, \mathbf{C})$ .

### 3.2. Framework Overview

We propose a hybrid generative framework to model the conditional probability distribution  $P(\mathbf{X}_{\text{pred}} | \mathbf{X}_{\text{hist}}, \mathbf{C})$  by coupling pre-trained LLMs with flow-matching mechanism. We first reconfigure pre-trained decoder-only LLMs into a native forecasting encoder-decoder backbone by modifying only the attention topology. Specifically, we initialize the LLM encoder by reusing the pre-trained decoder parameters while replacing causal self-attention with bidirectional self-attention. The LLM decoder keeps causal self-attention to preserve temporal causality, and introduces a newly added cross-attention that queries the encoder hidden states as keys and values. To capture stochastic continuous dynamics with the causal representation generation, we incorporate a continuous flow-matching mechanism conditioned on the LLM-generated representation. Specifically, we define a probability path and train a flow-matching denoising decoder to predict the corresponding temporal velocity field. Moreover, by learning an interval-conditioned average velocity, the temporal evolution can approximate the entire transport process within a single step, which enables efficient sampling without iterative denoising. During inference, each patch is produced autoregressively and sampled efficiently via one-step generation with low-latency.

### 3.3. Coupled Training

**Autoregressive Language Encoder-Decoder.** We first train the backbone to perform autoregressive encoder–decoder generation, producing semantically grounded and causal representations that serve as conditions for subsequent continuous flow-matching mechanism. Unlike conventional decoder-only LLMs that rely solely on causal attention, time series forecasting requires both bidirectional understanding and causal generation. To meet these two requirements, we reconfigure decoder-only LLMs into a native forecasting encoder-decoder backbone by modifying only the attention topology: the encoder adopts bidirectional self-attention to fuse the look-back window and context features, while the decoder preserves causal self-attention to generate future representations autoregressively. Given context features  $\mathbf{C}$ , we obtain text embeddings  $\mathbf{h}_{\text{enc.in}} \in \mathbb{R}^{M \times D_{\text{model}}}$  using the LLM’s native tokenizer and embedding layer. In parallel, the look-back window  $\mathbf{X}_{\text{hist}} \in \mathbb{R}^{L \times D}$  is partitioned into  $N = L/P$  non-overlapping patches  $\mathbf{x}_{1:N}$ , and projected into the same latent dimension  $D_{\text{model}}$  via a learnable linear layer to yield historical patch embeddings  $\mathbf{h}_{1:N}^{\text{enc.in}}$ . We then concatenate the text and patch embeddings along the sequence dimension and feed them into the bidirectional encoder to obtain fused contextual states  $\mathbf{h}^{\text{enc.out}}$ :

$$\mathbf{h}^{\text{enc.out}} = \text{Encoder}(\text{Concat}(\mathbf{h}_{\text{enc.in}}, \mathbf{h}_{1:N}^{\text{enc.in}})). \quad (1)$$

To generate future structures in a forecasting-native manner, we similarly segment the predicted window  $\mathbf{Y} \in \mathbb{R}^{H \times D}$  into patches  $\mathbf{y}_{1:N}$  and map them into latent embeddings

$\mathbf{z}_{1:N}$ . To align with autoregressive training and ensure strict causality, we employ a shifted-input strategy by prepending a learnable begin-of-sequence (BOS) embedding and excluding the final patch embedding  $\mathbf{z}_{1:N}^{\text{dec,in}}$ :

$$\mathbf{z}_{1:N}^{\text{dec,in}} = \text{Concat}(\text{BOS}, \mathbf{z}_{1:N-1}). \quad (2)$$

The shifted embeddings are then fed into the causal decoder, which combines (i) causal self-attention to model temporal dependencies without look-ahead and (ii) cross-attention over  $\mathbf{h}^{\text{enc,out}}$  to incorporate multimodal historical context. The resulting autoregressive states  $\mathbf{z}_{1:N}^{\text{dec,out}}$  are:

$$\mathbf{z}_{1:N}^{\text{dec,out}} = \text{Decoder}(\mathbf{z}_{1:N}^{\text{dec,in}}, \mathbf{h}^{\text{enc,out}}). \quad (3)$$

Notably, each  $\mathbf{z}_j^{\text{dec,out}}$  is computed under a strict causal mask and summarizes information only from  $\mathbf{y}_{1:j-1}$  together with the encoded history, making it a valid autoregressive representation for step- $j$  forecasting. These hidden states condition the subsequent continuous flow-matching mechanism, enabling the overall framework to jointly model semantic understanding and continuous stochastic dynamics.

**Continuous Flow-Matching Mechanism.** In contrast to standard diffusion (Wang & He, 2025; Chen et al., 2024) or flow-matching methods (Geng et al., 2025a;b; Lu et al., 2025; 2026) that estimate an instantaneous vector field at a single time point, our formulation explicitly models the average velocity over a finite time interval. By learning the dynamics across an integration window, the model can capture trajectory curvature more effectively, enabling high-quality generation with substantially fewer sampling steps. To construct a probability path that transports samples from a source distribution to the target distribution, we adopt a direct linear interpolation between the clean future patches  $\mathbf{y}_{1:N}$  and Gaussian noise  $\epsilon \sim \mathcal{N}(0, \mathbf{I})$ . For any time  $t \in [0, 1]$ , the intermediate noisy state  $\hat{\mathbf{y}}_{1:N}$  is defined as a convex combination of signal and noise:

$$\hat{\mathbf{y}}_{1:N} = (1 - t)\epsilon + t\mathbf{y}_{1:N}. \quad (4)$$

Here,  $t = 0$  corresponds to pure noise, while  $t = 1$  recovers the clean patches. Geometrically, this linear interpolation induces a straight-line trajectory in data space, characterized by a constant base velocity direction  $\mathbf{v}$ :

$$\mathbf{v} = \mathbf{y}_{1:N} - \epsilon. \quad (5)$$

This constant-velocity property substantially simplifies the underlying flow dynamics and provides a principled basis for high-quality few-step (and even one-step) generative modeling. We first project the interpolated noisy patches into the latent space using a linear projection layer, yielding the noised embeddings  $\hat{\mathbf{z}}_{1:N}^{\text{in}}$ . The denoising decoder strictly enforces the autoregressive constraint through a alignment

strategy: the noised embeddings  $\hat{\mathbf{z}}_{1:N}^{\text{in}}$  are used as queries, while the conditional hidden states  $\mathbf{z}_{1:N}^{\text{dec,out}}$  are used as keys and values. Notably, due to the shifted-input mechanism in the backbone, each context state  $\mathbf{z}_j^{\text{dec,out}}$  has already aggregated information from preceding clean patches  $\mathbf{y}_{1:j-1}$ . Unlike conventional flow matching, our estimator is conditioned not only on the current time  $t$  but also on a target step  $r$  (with  $r > t$ ), enabling the model to explicitly perceive the integration interval length. The velocity prediction for the  $j$ -th patch is thus formulated as:

$$\mathbf{u}_j^{\text{out}} = \text{DenoisingDecoder}(\hat{\mathbf{z}}_j^{\text{in}}, t, r, \mathbf{z}_{1:j}^{\text{dec,out}}), \quad (6)$$

where the denoising decoder serves as a velocity estimator. This formulation ensures that the predicted velocity  $\mathbf{u}_j^{\text{out}}$  depends only on the noised embedding  $\hat{\mathbf{z}}_j^{\text{in}}$ , the interval  $[t, r]$ , and the available autoregressive context  $\mathbf{z}_{1:j}^{\text{dec,out}}$ , thereby preventing any information leakage from future positions.

**Optimization Objective.** To explicitly guide the model to learn the average velocity along the temporal trajectory, we employ a Jacobian-Vector Product (JVP) corrected optimization objective. During training, we sample the current time step  $t \sim \mathcal{U}[0, 1]$  and a target time step  $r \sim \mathcal{U}[t, 1]$ . To approximate the true average velocity required to span the interval  $[t, r]$ , we apply a first-order Taylor expansion correction using the gradient of the velocity field. The final objective minimizes the mean squared error (MSE) between the predicted velocity  $\mathbf{u}$  and the JVP-corrected target. Formally, the loss function is expressed as:

$$\mathbb{E}_{t, r, \epsilon, \mathbf{y}} \left[ \frac{1}{N} \sum_{j=1}^N \left\| \mathbf{u}_j^{\text{out}} - \left( \mathbf{v}_j - (r - t) \frac{\partial \mathbf{u}_j^{\text{out}}}{\partial t} \right) \right\|_2^2 \right], \quad (7)$$

where  $\frac{\partial \mathbf{u}_j^{\text{out}}}{\partial t}$  denotes the time partial derivative of the velocity field, which is efficiently computed via JVP. Minimizing this objective explicitly penalizes velocity variations, thereby compelling the model to learn straight temporal trajectories.

### 3.4. One-step Inference

**Autoregressive Patch Generation.** As illustrated in Figure 1 (Right), inference proceeds iteratively in an autoregressive manner. For generating the  $j$ -th patch, the previously generated patches  $\hat{\mathbf{y}}_{1:j-1}$  are first appended to the predicted window, which initiates with the BOS token. This sequential appending serves to update the conditional keys and values used by the decoder, effectively capturing the causal dependencies between continuous temporal intervals. Unlike traditional point-regression models, our autoregressive appending maintains global semantic coherence by leveraging the hidden states of previously generated patches as contextual conditions for the subsequent generation step.

**One-step Generative Modeling.** Within each autoregressive step, we initiate the generation of the  $j$ -th patch by sampling a pure Gaussian noise patch  $\mathbf{y}_j^{(0)} \sim \mathcal{N}(0, \mathbf{I})$  (labeled as  $\mathbf{y}^{(0)}$  in Figure 1). This noise patch is projected into the latent space via a linear layer to obtain the noisy representation  $\mathbf{z}_j^{(0)}$ . Given the current noisy representation and the available autoregressive context, the denoising decoder functions as a velocity estimator and predicts the interval-conditioned patch-level velocity field. Notably, by learning an interval-conditioned average velocity, the transport process can approximate the entire transformation from noise ( $t = 0$ ) to clean prediction ( $t = 1$ ) within a single step, which enables efficient sampling without iterative denoising. The output  $\mathbf{y}_j^{\text{out}}$  is then recovered by integrating the predicted velocity over the time interval as shown in Eq. (8):

$$\mathbf{y}_j^{\text{out}} = \mathbf{y}_j^{(0)} + \int_0^1 \mathbf{u}(\mathbf{z}_\tau, \tau, \mathbf{z}_{1:j}^{\text{dec,out}}) d\tau. \quad (8)$$

Finally, the integrated result serves as the generated patch  $\hat{\mathbf{y}}_j$  and is appended to the predicted window to form  $\hat{\mathbf{y}}_{1:j}$ , which will be used as the input context for the next autoregressive inference step. Notably, this one-step generation, corresponding to a single function evaluation, reduces inference latency while maintaining high-performance forecasting.

## 4. Experiments

In this section, we conduct comprehensive experiments to evaluate the performance of our proposed CoGenCast on multiple benchmark datasets. Additionally, we perform extensive ablation studies and exploration analysis.

### 4.1. Experimental Setup

**Datasets.** We conduct extensive experiments on publicly available datasets, specifically including Energy (Liu et al., 2024a), ETT (4 subsets) (Zhou et al., 2021), Environment (abbreviated as Environ.) (Liu et al., 2024a), Exchange (Wu et al., 2021), Health (Liu et al., 2024a), Wind (Li et al., 2022), and Solar (Lai et al., 2018). Detailed statistics are summarized in Table 1. To clearly illustrate the practical scenarios and scale of these datasets, the table provides an overview of each dataset’s domain, the number of samples, and the number of variables per sample. A more comprehensive description can be found in Appendix A.

**Baselines.** To ensure a comprehensive evaluation, we compare our method with eight representative baselines spanning three major categories. First, for LLM-based methods, we select LLM4TS (Chang et al., 2025), which fine-tunes a pre-trained LLM using multi-scale temporal encoding, and Time-LLM (Jin et al., 2023), which reprograms frozen LLMs to align time series data with textual prototypes. Second, we select generative-based methods such

Table 1. Overview of the dataset statistics, including domain, the number of samples, and the number of variables per sample.

DATASETS	DOMAIN	VARIABLES	LENGTH
Energy	Energy	1	1479
ETTh1	Energy	7	17420
ETTh2	Energy	7	17420
ETTm1	Energy	7	69680
ETTm2	Energy	7	69680
Environment	Environment	1	11102
Exchange	Finance	8	7588
Health	Health	1	1389
Wind	Electricity	7	48673
Solar	Electricity	137	52560

as FlowTS (Hu et al., 2024), CDPM (Zhang et al., 2024a) and CSDI (Tashiro et al., 2021). FlowTS constructs a continuous probability path using flow-matching, CDPM employs conditional diffusion probabilistic models, and CSDI uses a conditional score-based diffusion process to model the data distribution. Third, we compare with transformer-based methods, including TimeDART (Wang et al., 2024), PatchTST (Nie et al., 2022) and Autoformer (Wu et al., 2021). Further details are provided in Appendix B.1.

**Implementation Details.** In the experiments, for all datasets, we set the look-back window length to  $L = 96$  and the predicted window length with  $H \in \{12, 24, 36, 48\}$ . We report two widely used forecasting metrics: mean squared error (MSE) and mean absolute error (MAE). Our backbone architecture is initialized with the pre-trained Qwen3-0.6B model parameters for both the encoder and decoder. For the continuous flow-matching mechanism, we adopt a linear noise scheduler, which naturally matches our straight-trajectory formulation and enables efficient one-step sampling at inference time. A more comprehensive implementation details can be found in Appendix B.2.

### 4.2. Main Results

Table 2 summarizes the main forecasting results across ten real-world benchmarks datasets. Overall, CoGenCast achieves the consistent and competitive performance, delivering the best results across most datasets, which demonstrates strong generation capability across diverse domains. In particular, our approach outperforms representative LLM-based baselines (LLM4TS and Time-LLM), as well as strong generative-based and transformer-based methods, suggesting that effective forecasting benefits from simultaneously capturing semantic understanding and continuous stochastic dynamics. On average, we observe an approximate 11% reduction in MSE compared to LLM-based approaches and over 7% improvement over strong transformer-

Table 2. Time series forecasting results. All results are averaged Mean Squared Error (MSE) and Mean Absolute Error(MAE) from the same look-back window of  $L = 96$  and 4 different predicted windows of  $\{12, 24, 36, 48\}$ . The best results are in **bold** and the second best are underlined. Full results are detailed in Appendix C.

METHODS	OURS	LLM-BASED				GENERATIVE-BASED						TRANSFORMER-BASED					
		LLM4TS		Time-LLM		FlowTS		CDPM		CSDI		TimeDART		PatchTST		Autoformer	
METRICS	MSE	MAE	MSE	MAE	MSE	MAE	MSE	MAE	MSE	MAE	MSE	MSE	MAE	MSE	MAE	MSE	MAE
Energy	<b>0.290</b> <b>0.390</b>	0.325	0.424	<u>0.318</u> <u>0.413</u>	0.418	0.473	0.373	0.447	0.669	0.634	0.323	0.421	0.327	0.424	0.506	0.542	
ETTh1	<b>0.324</b> <b>0.366</b>	<u>0.348</u> <u>0.382</u>	0.364	0.391	0.381	0.413	0.350	0.383	1.355	0.959	0.354	0.384	0.367	0.390	0.495	0.469	
ETTh2	0.159 <b>0.246</b>	0.195	0.281	0.206	0.291	0.218	0.300	0.193	0.279	0.647	0.566	<u>0.145</u>	0.253	<b>0.142</b>	<u>0.251</u>	0.192	0.301
ETTm1	<b>0.221</b> <b>0.283</b>	0.253	0.314	0.304	0.349	0.327	0.374	0.302	0.352	0.898	0.648	<u>0.240</u>	<u>0.309</u>	0.243	0.312	0.375	0.432
ETTm2	<b>0.109</b> <b>0.200</b>	0.145	0.252	0.141	0.247	0.197	0.305	0.191	0.300	0.938	0.710	<u>0.122</u>	<u>0.232</u>	0.126	0.235	0.238	0.365
Environ.	<b>0.297</b> <b>0.377</b>	0.316	<u>0.395</u>	0.320	0.400	0.349	0.425	0.334	0.419	1.249	0.883	0.314	0.399	<u>0.309</u>	0.397	0.366	0.461
Exchange	<b>0.030</b> <b>0.117</b>	0.037	0.133	0.035	0.130	0.061	0.185	0.046	0.153	0.628	0.656	0.034	<u>0.127</u>	<u>0.033</u>	<u>0.127</u>	0.087	0.214
Health	<b>1.422</b> <b>0.804</b>	1.679	0.923	1.611	0.887	1.736	0.943	1.591	0.897	2.218	1.271	<u>1.510</u>	<u>0.852</u>	1.540	0.857	1.828	1.018
Wind	<b>0.527</b> <b>0.423</b>	0.591	0.484	0.543	0.444	0.651	0.497	0.583	0.468	0.908	0.650	0.542	0.443	<u>0.539</u>	<u>0.441</u>	0.830	0.609
Solar	<b>0.221</b> <b>0.287</b>	0.239	0.307	0.233	0.299	0.369	0.422	0.350	0.410	0.965	0.786	0.236	0.301	<u>0.232</u>	<u>0.298</u>	0.661	0.626

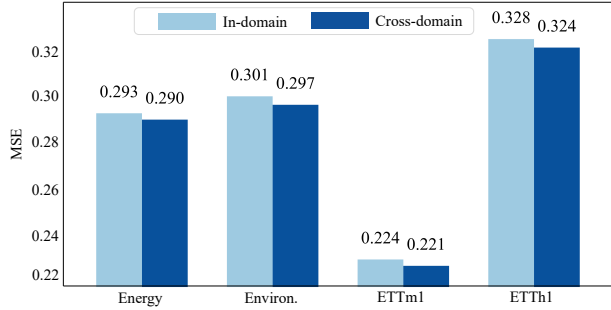


Figure 2. Performance comparison between in-domain and cross-domain training. The bar chart shows the MSE reduction achieved by cross-domain training across four representative benchmarks.

based baselines (e.g., PatchTST), indicating that the gains stem from a coupled modeling of both structural dependencies and temporal dynamics rather than architectural scaling alone. In summary, CoGenCast delivers state-of-the-art results with high consistency. This advantage is enabled by structurally reconfiguring pre-trained decoder-only LLMs into a native forecasting encoder-decoder backbone via attention topology modification, and further integrating a flow-matching generative mechanism to model continuous stochastic dynamics conditioned on autoregressively generated representations. In addition to the in-domain evaluation in Table 2, we further conduct a general cross-domain training setting to strengthen the generalization capability of our framework. As shown in Figure 2, cross-domain training leads to consistent performance improvements compared to training within a single domain, reducing MSE across multiple datasets (e.g., Energy, Environ., ETTm1, and ETTh1). These experimental results validate the effectiveness of our proposed CoGenCast. Visualized results are provided in Appendix H, and the full results can be found in Appendix C.

Table 3. Ablation study on the encoder-decoder architecture. We compare the forecasting performance of our full model with encoder-only and decoder-only variants.

METHODS	ENERGY		ENVIRON.		EXCHANGE		WIND	
	MSE	MAE	MSE	MAE	MSE	MAE	MSE	MAE
Ours	<b>0.293</b>	<b>0.395</b>	<b>0.301</b>	<b>0.381</b>	<b>0.031</b>	<b>0.118</b>	<b>0.532</b>	<b>0.425</b>
Encoder-only	0.331	0.431	0.313	0.404	0.036	0.132	0.547	0.453
Decoder-only	0.953	0.742	0.602	0.574	0.188	0.255	2.010	0.833

### 4.3. Ablation Study

**Encoder-Decoder Variants.** To verify the effectiveness of our encoder-decoder architecture, we conduct experiments with encoder-decoder variants. For the encoder-only variant, we retain the former encoder and add a linear layer at the end of the model. For the decoder-only variant, we retain the latter decoder and the denoising decoder. As shown in Table 3, the full encoder-decoder architecture achieves superior results compared to both variants on all datasets. Notably, the significant performance degradation in the decoder-only variant underscores the critical role of the encoder in providing semantic conditioning for the generative process. Meanwhile, the performance gap between the full architecture and the encoder-only variant verifies that integrating flow matching into the autoregressive optimization captures continuous dynamics more effectively than a linear layer. Overall, these results confirm that combining bidirectional context modeling in the encoder with causal representation generation in the decoder is necessary, and the proposed encoder-decoder architecture is essential to achieve the superior forecasting performance.

**Ablation on AR-Flow.** Table 4 presents the ablation study results to evaluate the individual contributions of the au-

Table 4. Ablation study on the generative components. We evaluate the individual contributions of the autoregressive (AR) and the flow-matching mechanism.

METHODS METRICS	ENERGY		ETTH1		ETTM1		WIND	
	MSE	MAE	MSE	MAE	MSE	MAE	MSE	MAE
<b>Ours</b>	<b>0.293</b>	<b>0.395</b>	<b>0.328</b>	<b>0.367</b>	<b>0.224</b>	<b>0.285</b>	<b>0.532</b>	<b>0.425</b>
w/o AR	0.343	0.429	0.369	0.404	0.260	0.324	0.693	0.513
w/o Flow	0.335	0.422	0.358	0.396	0.251	0.317	0.611	0.482
w/o AR-Flow	0.345	0.430	0.372	0.406	0.262	0.327	0.711	0.522

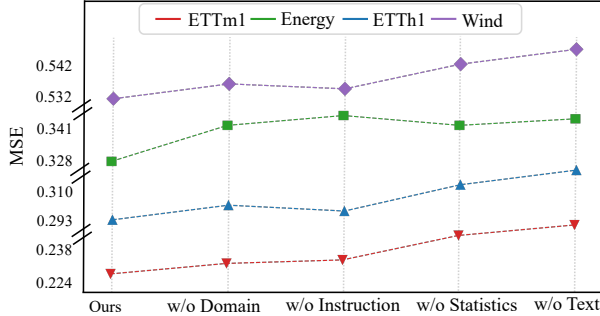


Figure 3. Ablation study on context features. We evaluate the impact of removing domain knowledge, task instruction, statistics information, and the entire textual input on forecasting performance.

toregressive mechanism and the flow-matching mechanism. We compare the full model with three variants: w/o AR, w/o Flow and w/o AR-Flow. The results clearly show that removing either component leads to a significant degradation in forecasting accuracy. Specifically, the w/o AR variant exhibits a substantial increase in MSE, confirming that LLM-based semantic understanding is crucial for capturing long-term contextual dependencies. Simultaneously, the w/o Flow variant performs worse than the full model, validating that the flow-matching mechanism effectively models the continuous temporal dynamics in time series data. Ultimately, the full model achieves the best performance by successfully coupling these two methods.

**Ablation on Context Features.** As shown in Figure 3, to investigate the impact of specific context features on forecasting performance, we conduct a detailed ablation study. The considered variants include removing the entire textual input (w/o Text), as well as selectively excluding domain knowledge (w/o Domain), task instruction (w/o Instruction), and statistics information (w/o Statistics). The results indicate that the complete text-guided framework consistently yields the best performance. This confirms that the incorporation of context features provides essential guidance, effectively enhancing forecasting accuracy. Notably, removing the statistics information generally leads to a more pronounced error increase compared to other sub-components, further confirming its effectiveness and necessity.

Table 5. Comparative analysis against generative baselines. The results demonstrate the superior performance of our method compared to vanilla flow-matching and diffusion models.

METHODS METRICS	ENERGY		ENVIRON.		ETTH1		EXCHANGE	
	MSE	MAE	MSE	MAE	MSE	MAE	MSE	MAE
<b>Ours</b>	<b>0.293</b>	<b>0.395</b>	<b>0.301</b>	<b>0.381</b>	<b>0.328</b>	<b>0.367</b>	<b>0.031</b>	<b>0.118</b>
Flow-matching	0.332	0.418	0.329	0.399	0.372	0.399	0.051	0.131
Diffusion	0.325	0.413	0.322	0.395	0.363	0.394	0.046	0.127

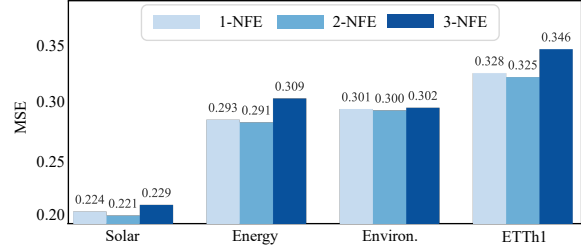


Figure 4. Comparative analysis on the number of function evaluations (NFE). We compare the forecasting performance across 1, 2, and 3 sampling steps.

#### 4.4. Comparison with Generative Models

**Comparison with Generative Models.** To further evaluate the architectural advantages of our approach, we conduct a comparative study by replacing our generation module with vanilla diffusion and flow-matching components within the identical framework. As demonstrated in Table 5, our method achieves superior forecasting performance across all benchmarks. This advantage is primarily attributed to the fundamental differences in modeling objectives. While diffusion models rely on complex iterative denoising to recover signals and standard flow-matching models targets instantaneous velocity, our method explicitly models the average velocity connecting the prior to the ground truth.

**Efficiency-Performance Trade-off.** As shown in Figure 4, we investigate the impact of the number of function evaluations (NFE) on forecasting performances. Remarkably, one-step (1-NFE) generation achieves performance parity with the optimal 2-NFE, whereas extending the inference to 3-NFE results in slight marginal degradation. This confirms that our learned temporal trajectories are nearly linear, making a single Euler step sufficient for high-precision generation. Additional steps become redundant and prone to numerical error accumulation. Therefore, we adopt 1-NFE to achieve the best trade-off, ensuring real-time inference speed without compromising performance.

#### 4.5. Hyperparameter Sensitivity

**Patch Size.** As visualized in Figure 5, we investigate the impact of patch size on forecasting performance. The results demonstrate that different datasets exhibit varying levels of

**Table 6.** Performance comparison across different backbone architectures. We evaluate the impact of backbone by comparing the Qwen family (0.6B, 1.7B, 4B) with a vanilla Transformer.

BACKBONE METRICS	ENERGY		ENVIRON.		EXCHANGE		WIND	
	MSE	MAE	MSE	MAE	MSE	MAE	MSE	MAE
Transformer	0.301	0.399	0.311	0.388	0.037	0.123	0.587	0.461
Qwen3-0.6B	0.293	0.395	0.301	0.381	0.031	0.118	0.532	0.425
Qwen3-1.7B	0.295	0.396	0.300	0.380	0.031	0.117	0.530	0.424
Qwen3-4B	0.290	0.392	0.297	0.376	0.029	0.115	0.525	0.417

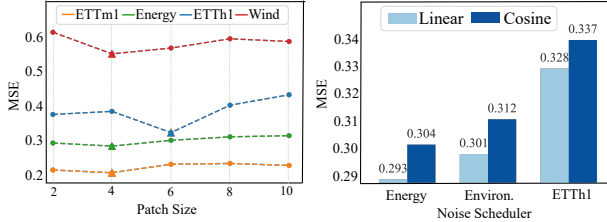


**Figure 5.** Hyperparameter sensitivity analysis. (Left) Impact of varying patch sizes on MSE across different datasets. (Right) Performance comparison between linear and cosine noise schedules.

sensitivity to this hyperparameter. Notably, neither an overly small nor an excessively large patch size is desirable. This is attributed to the fact that the former fails to capture sufficient local semantic context, while the latter risks smoothing out fine-grained temporal dynamics. Thus, selecting a suitable patch size is essential to the forecasting performance.

**Noise Scheduler.** We investigate the impact of different noise scheduler strategies on forecasting performance, comparing linear and cosine schedulers. As shown in Figure 5, the linear scheduler yields superior results across most datasets. This is attributed to the linear scheduler offering uniform discretization that perfectly aligns with our average velocity modeling, which implies a straight constant-speed trajectory. Crucially, this alignment is significantly more suitable for our one-step generation modeling, as it ensures precise inference in a single step without the unnecessary temporal curvature introduced by the cosine scheduler.

#### 4.6. Analysis Experiment

**LLM Backbone.** To verify the effectiveness of the backbone architecture, we conduct a comparative analysis between a vanilla Transformer and the Qwen LLM family across different parameter scales, as shown in Table 6. The results demonstrate that LLM-based backbones significantly outperform the vanilla Transformer backbone. This is attributed to the LLMs' stronger fitting capability and the integration of multi-modal context features, which provide deeper semantic understanding to explicitly condition the generation process. Notably, comparing within the Qwen family, the Qwen3-4B model achieves the best performance.

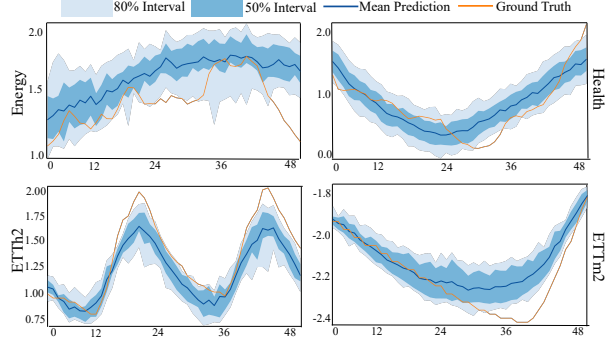


**Figure 6.** Forecasting with uncertainty on four datasets. The plots compare the ground truth trajectories with the model’s mean predictions, along with the 50% and 80% predictive intervals.

However, the performance gap between the 0.6B and 4B models is marginal. Considering the comprehensive trade-off between computational resources, training time, and forecasting performance, we selected Qwen3-0.6B as our default backbone, as it delivers performance approaching SOTA levels with significantly higher efficiency.

**Generative Uncertainty.** To validate the uncertainty modeling capabilities of our framework, we visualize the different predictive distributions in Figure 6. The results demonstrate that our method generates forecasting distributions that closely align with the ground truth, with the 50% and 80% confidence intervals effectively encompassing the inherent data variability. This high degree of overlap clearly indicates that our model provides not only precise point estimates but also well-calibrated uncertainty quantification. Such reliability suggests that our approach excels at capturing the stochastic nature of time series, offering significant practical potential for uncertainty-aware forecasting.

## 5. Conclusion

In this paper, we propose CoGenCast, a hybrid generative framework that couples pre-trained LLMs with flow-matching mechanism for effective time series forecasting. This bridges the critical gap between semantic understanding and continuous stochastic modeling. By reconfiguring pre-trained decoder-only LLMs into a native forecasting encoder-decoder backbone, we leverage the comprehensive contextual understanding to condition the flow-matching generation process. Our approach linearizes the generative dynamics, establishing a direct and stable temporal trajectory that can be solved efficiently with a single function evaluation. Extensive experiments on ten benchmark datasets show that CoGenCast consistently outperforms previous compared baselines, confirming its effectiveness. Finally, we hope that this work offers a valuable and inspiring perspective for future time series forecasting methods.

## Impact Statement

This paper introduces a hybrid generative framework that couples pre-trained LLMs with flow-matching mechanism for effective time series forecasting. Our work offers valuable insights for future research in the synergy between LLMs and continuous probabilistic generation. Experimental results demonstrate the effectiveness of our method and its potential real-world applicability. We have ensured that all datasets used in the experiments are publicly available, and we have carefully considered the ethical implications of our work. Therefore, we believe that our research does not present any ethical or moral risks.

## References

Bian, Y., Ju, X., Li, J., Xu, Z., Cheng, D., and Xu, Q. Multi-patch prediction: Adapting llms for time series representation learning. *arXiv preprint arXiv:2402.04852*, 2024.

Chang, C., Wang, W.-Y., Peng, W.-C., and Chen, T.-F. Llm4ts: Aligning pre-trained llms as data-efficient time-series forecasters. *ACM Transactions on Intelligent Systems and Technology*, 16(3):1–20, 2025.

Chen, X., Liu, Z., Xie, S., and He, K. Deconstructing denoising diffusion models for self-supervised learning. *arXiv preprint arXiv:2401.14404*, 2024.

Cheng, M., Zhang, J., Liu, Z., Liu, C., and Xie, Y. Hmf: A hybrid multi-factor framework for dynamic intraoperative hypotension prediction. *arXiv e-prints*, pp. arXiv–2409, 2024.

Cheng, M., Liu, Z., Tao, X., Liu, Q., Zhang, J., Pan, T., Zhang, S., He, P., Zhang, X., Wang, D., et al. A comprehensive survey of time series forecasting: Concepts, challenges, and future directions. *Authorea Preprints*, 2025a.

Cheng, M., Tao, X., Liu, Q., Zhang, H., Chen, Y., and Lian, D. Cross-domain pre-training with language models for transferable time series representations. In *Proceedings of the Eighteenth ACM International Conference on Web Search and Data Mining*, pp. 175–183, 2025b.

Cheng, M., Wang, J., Wang, D., Tao, X., Liu, Q., and Chen, E. Can slow-thinking llms reason over time? empirical studies in time series forecasting. *arXiv preprint arXiv:2505.24511*, 2025c.

Feng, F., He, X., Wang, X., Luo, C., Liu, Y., and Chua, T.-S. Temporal relational ranking for stock prediction. *ACM Transactions on Information Systems (TOIS)*, 37(2):1–30, 2019.

Geng, Z., Deng, M., Bai, X., Kolter, J. Z., and He, K. Mean flows for one-step generative modeling. *arXiv preprint arXiv:2505.13447*, 2025a.

Geng, Z., Lu, Y., Wu, Z., Shechtman, E., Kolter, J. Z., and He, K. Improved mean flows: On the challenges of fastforward generative models. *arXiv preprint arXiv:2512.02012*, 2025b.

Gruver, N., Finzi, M., Qiu, S., and Wilson, A. G. Large language models are zero-shot time series forecasters. *Advances in Neural Information Processing Systems*, 36: 19622–19635, 2023.

Guo, X., Zhang, Y., Chen, B., Xu, H., Wang, J., and Long, M. Dynamical diffusion: Learning temporal dynamics with diffusion models. *arXiv preprint arXiv:2503.00951*, 2025.

Hu, Y., Wang, X., Ding, Z., Wu, L., Zhang, H., Li, S. Z., Wang, S., Zhang, J., Li, Z., and Chen, T. Flows: Time series generation via rectified flow. *arXiv preprint arXiv:2411.07506*, 2024.

Jiang, Y., Chen, Y., Li, X., Chao, Q., Liu, S., and Cong, G. Fstllm: Spatio-temporal llm for few shot time series forecasting. In *Forty-second International Conference on Machine Learning*.

Jin, M., Wang, S., Ma, L., Chu, Z., Zhang, J. Y., Shi, X., Chen, P.-Y., Liang, Y., Li, Y.-F., Pan, S., et al. Time-llm: Time series forecasting by reprogramming large language models. *arXiv preprint arXiv:2310.01728*, 2023.

Jin, M., Zhang, Y., Chen, W., Zhang, K., Liang, Y., Yang, B., Wang, J., Pan, S., and Wen, Q. Position: What can large language models tell us about time series analysis. In *41st International Conference on Machine Learning*. MLResearchPress, 2024.

Kollovieh, M., Lienen, M., Lüdke, D., Schwinn, L., and Günemann, S. Flow matching with gaussian process priors for probabilistic time series forecasting. *arXiv preprint arXiv:2410.03024*, 2024.

Lai, G., Chang, W.-C., Yang, Y., and Liu, H. Modeling long-and short-term temporal patterns with deep neural networks. In *The 41st international ACM SIGIR conference on research & development in information retrieval*, pp. 95–104, 2018.

Li, Y., Lu, X., Wang, Y., and Dou, D. Generative time series forecasting with diffusion, denoise, and disentanglement. *Advances in Neural Information Processing Systems*, 35: 23009–23022, 2022.

Liu, H., Xu, S., Zhao, Z., Kong, L., Prabhakar Kamarthi, H., Sasanur, A., Sharma, M., Cui, J., Wen, Q., Zhang,

C., et al. Time-mmd: Multi-domain multimodal dataset for time series analysis. *Advances in Neural Information Processing Systems*, 37:77888–77933, 2024a.

Liu, H., Zhao, Z., Wang, J., Kamarthi, H., and Prakash, B. A. Lstprompt: Large language models as zero-shot time series forecasters by long-short-term prompting. *arXiv preprint arXiv:2402.16132*, 2024b.

Liu, Z., Cheng, M., Li, Z., Huang, Z., Liu, Q., Xie, Y., and Chen, E. Adaptive normalization for non-stationary time series forecasting: A temporal slice perspective. *Advances in Neural Information Processing Systems*, 36: 14273–14292, 2023.

Liu, Z., Yang, J., Cheng, M., Luo, Y., and Li, Z. Generative pretrained hierarchical transformer for time series forecasting. In *Proceedings of the 30th ACM SIGKDD conference on knowledge discovery and data mining*, pp. 2003–2013, 2024c.

Lu, Y., Sun, Q., Wang, X., Jiang, Z., Zhao, H., and He, K. Bidirectional normalizing flow: From data to noise and back. *arXiv preprint arXiv:2512.10953*, 2025.

Lu, Y., Lu, S., Sun, Q., Zhao, H., Jiang, Z., Wang, X., Li, T., Geng, Z., and He, K. One-step latent-free image generation with pixel mean flows. *arXiv preprint arXiv:2601.22158*, 2026.

Luo, Y., Zhou, Y., Cheng, M., Wang, J., Wang, D., Pan, T., and Zhang, J. Time series forecasting as reasoning: A slow-thinking approach with reinforced llms. *arXiv preprint arXiv:2506.10630*, 2025.

Moghadas, S. M., Cornelis, B., and Munteanu, A. Frèqflow: Long-term forecasting using lightweight flow matching. *arXiv preprint arXiv:2511.16426*, 2025.

Nie, Y., Nguyen, N. H., Sinthong, P., and Kalagnanam, J. A time series is worth 64 words: Long-term forecasting with transformers. arxiv 2022. *arXiv preprint arXiv:2211.14730*, 2022.

Niu, W., Xie, Z., Sun, Y., He, W., Xu, M., and Hao, C. Langtime: A language-guided unified model for time series forecasting with proximal policy optimization. *arXiv preprint arXiv:2503.08271*, 2025.

Pan, Z., Jiang, Y., Garg, S., Schneider, A., Nevyvaka, Y., and Song, D.  $s^2$  ip-llm: Semantic space informed prompt learning with llm for time series forecasting. In *Forty-first International Conference on Machine Learning*, 2024.

Rasul, K., Seward, C., Schuster, I., and Vollgraf, R. Autoregressive denoising diffusion models for multivariate probabilistic time series forecasting. In *International conference on machine learning*, pp. 8857–8868. PMLR, 2021.

Shen, L. and Kwok, J. Non-autoregressive conditional diffusion models for time series prediction. In *International Conference on Machine Learning*, pp. 31016–31029. PMLR, 2023.

Tao, X., Zhang, S., Cheng, M., Wang, D., Pan, T., Pan, B., Zhang, C., and Wang, S. From values to tokens: An llm-driven framework for context-aware time series forecasting via symbolic discretization. *arXiv preprint arXiv:2508.09191*, 2025.

Tashiro, Y., Song, J., Song, Y., and Ermon, S. Csd: Conditional score-based diffusion models for probabilistic time series imputation. *Advances in neural information processing systems*, 34:24804–24816, 2021.

Wang, D., Cheng, M., Liu, Z., and Liu, Q. Timedart: A diffusion autoregressive transformer for self-supervised time series representation. *arXiv preprint arXiv:2410.05711*, 2024.

Wang, R. and He, K. Diffuse and disperse: Image generation with representation regularization. *arXiv preprint arXiv:2506.09027*, 2025.

Wu, H., Xu, J., Wang, J., and Long, M. Autoformer: Decomposition transformers with auto-correlation for long-term series forecasting. *Advances in neural information processing systems*, 34:22419–22430, 2021.

Wu, X., Qiu, X., Gao, H., Hu, J., Yang, B., and Guo, C.  $k^2$  vae: A koopman-kalman enhanced variational autoencoder for probabilistic time series forecasting. *arXiv preprint arXiv:2505.23017*, 2025.

Xie, Z., Li, Z., He, X., Xu, L., Wen, X., Zhang, T., Chen, J., Shi, R., and Pei, D. Chatts: Aligning time series with llms via synthetic data for enhanced understanding and reasoning. *arXiv preprint arXiv:2412.03104*, 2024.

Xue, H. and Salim, F. D. Promptcast: A new prompt-based learning paradigm for time series forecasting. *IEEE Transactions on Knowledge and Data Engineering*, 36(11):6851–6864, 2023.

Ye, W., Xu, Z., and Gui, N. Non-stationary diffusion for probabilistic time series forecasting. *arXiv preprint arXiv:2505.04278*, 2025.

Zhang, J., Cheng, M., Tao, X., Liu, Z., and Wang, D. Conditional denoising meets polynomial modeling: A flexible decoupled framework for time series forecasting. *arXiv preprint arXiv:2410.13253*, 2024a.

Zhang, X. N., Pu, Y., Kawamura, Y., Loza, A., Bengio, Y., Shung, D., and Tong, A. Trajectory flow matching with applications to clinical time series modelling. *Advances in Neural Information Processing Systems*, 37:107198–107224, 2024b.

Zhou, H., Zhang, S., Peng, J., Zhang, S., Li, J., Xiong, H., and Zhang, W. Informer: Beyond efficient transformer for long sequence time-series forecasting. In *Proceedings of the AAAI conference on artificial intelligence*, volume 35, pp. 11106–11115, 2021.

Zhou, J., Lu, X., Xiao, Y., Tang, J., Su, J., Li, Y., Liu, J., Lyu, J., Ma, Y., and Dou, D. Sdwpf: a dataset for spatial dynamic wind power forecasting over a large turbine array. *Scientific Data*, 11(1):649, 2024.

## A. Dataset Description

To evaluate the effectiveness of our proposed framework, we conduct extensive experiments on 10 time series forecasting datasets. These datasets cover diverse domains, including energy, environment, finance, health and electricity. For detailed description of the datasets, please refer to Table 7.

Table 7. Full dataset descriptions. Samples are organized in (Train/Validation/Test).

DATASETS	LOOK-BACK	PREDICTED	VARIABLES	SAMPLES	DOMAIN	FREQUENCY
Energy	96	{12, 24, 36, 48}	1	928/138/284	Energy	1 Week
ETTh1	96	{12, 24, 36, 48}	7	8293/2869/2869	Energy	1 Hour
ETTh2	96	{12, 24, 36, 48}	7	8293/2869/2869	Energy	1 Hour
ETTm1	96	{12, 24, 36, 48}	7	34417/11473/11473	Energy	15 Mins
ETTm2	96	{12, 24, 36, 48}	7	34417/11473/11473	Energy	15 Mins
Environment	96	{12, 24, 36, 48}	1	10566/1515/3038	Environment	1 Day
Exchange	96	{12, 24, 36, 48}	8	4928/713/1470	Finance	1 Day
Health	96	{12, 24, 36, 48}	1	829/93/230	Health	1 Week
Wind	96	{12, 24, 36, 48}	7	33688/4821/9687	Electricity	15 Mins
Solar	96	{12, 24, 36, 48}	137	36445/5245/10501	Electricity	10 Mins

**Energy (Liu et al., 2024a)** This dataset comprises weekly U.S. gasoline price time series spanning from April 1993 to the present. The data is officially released by the U.S. Energy Information Administration (EIA)

**ETT(4 subsets) (Zhou et al., 2021)** This dataset comprises time series data of oil temperature and power load collected from electricity transformers spanning July 2016 to July 2018. It is divided into four subsets, each with different recording intervals: ETTh1 and ETTh2 have hourly recordings, while ETTm1 and ETTm2 are recorded every 15 minutes.

**Environment (Liu et al., 2024a)** This dataset comprises daily air quality time series collected from the U.S. EPA spanning the full available period, recorded at a daily frequency.

**Exchange (Wu et al., 2021)** This dataset collects the daily exchange rates of eight countries—Australia, the UK, Canada, Switzerland, China, Japan, New Zealand, and Singapore—from 1990 to 2016.

**Health (Liu et al., 2024a)** This dataset comprises weekly U.S. Influenza-Like Illness (ILI) statistics spanning from 1954 to the present, recorded at a weekly frequency. The accompanying data is collected from the CDC Weekly U.S. Influenza Surveillance Report, released weekly.

**Wind (Li et al., 2022)** This dataset comprises wind power measurements sampled every 15 minutes from 2020 to 2021.

**Solar (Lai et al., 2018)** This dataset records the solar power production of 137 PV plants in 2006, which are sampled every 10 minutes.

## B. Implementation Details

### B.1. Compared Baselines

To more comprehensively evaluate the capabilities of our proposed method, we compare our method with eight representative baselines in our experiments. Specifically, we include LLM-based approaches (LLM4TS and Time-LLM), generative-based models (FlowTS, CDPM, and CSDI), and transformer-based methods (TimeDART, PatchTST, and Autoformer).

**LLM4TS (Chang et al., 2025)** LLM4TS<sup>1</sup> is a framework that adapts pre-trained LLMs for time series forecasting via two-stage fine-tuning (time-series alignment and downstream forecasting) and a two-level multi-scale temporal aggregation mechanism, enabling LLMs to better capture time series characteristics and multi-resolution patterns, especially in data-scarce settings.

**Time-LLM (Jin et al., 2023)** Time-LLM<sup>2</sup> is a reprogramming framework that aligns time-series inputs with text prototypes and feeds them into a frozen LLM, enhanced by a Prompt-as-Prefix mechanism to guide temporal reasoning for forecasting.

**FlowTS (Hu et al., 2024)** FlowTS<sup>3</sup> is an ODE-based rectified-flow model that learns straight-line (geodesic) transport paths in probability space for efficient exact trajectory simulation, further enhanced with adaptive sampling and time-series decomposition plus global-context/positional modules to improve generation quality.

**CDPM (Zhang et al., 2024a)** CDPM<sup>4</sup> is a hybrid framework that decomposes time series into trend and seasonal components and trains a diffusion-based denoiser for stochastic seasonal fluctuations alongside an enhanced linear model for smooth trends, jointly optimized end-to-end to capture both complex dynamics and long-term structure.

**CSDI (Tashiro et al., 2021)** CSDI<sup>5</sup> is a conditional score-based diffusion model that learns the data distribution given observed entries via a denoising score network, enabling correlation-aware sampling to reconstruct missing values and produce probabilistic imputations.

**TimeDART (Wang et al., 2024)** TimeDART<sup>6</sup> is a self-supervised pre-training framework that combines causal transformer-based autoregressive modeling with a denoising diffusion process to jointly learn global trend evolution and fine-grained local patterns for transferable time-series representations.

**PatchTST (Nie et al., 2022)** PatchTST<sup>7</sup> is a patch-based, channel-independent Transformer that treats subseries patches as tokens and shares model weights across variables, greatly reducing attention cost while preserving local semantics to improve long-horizon forecasting and self-supervised representation learning.

**Autoformer (Wu et al., 2021)** Autoformer<sup>8</sup> is a decomposition-based forecasting architecture that embeds progressive trend/seasonal decomposition into the model and replaces self-attention with an Auto-Correlation mechanism to capture periodic dependencies and aggregate representations at the sub-series level for efficient long-horizon prediction.

## B.2. Implementation Details for Experiment

The look-back window length of  $L = 96$  and the predicted window lengths  $H \in \{12, 24, 36, 48\}$  were applied to all datasets. To ensure consistency, a batch size of 4 and a channel-independent configuration were applied across all datasets. We employed the Adam optimizer with an initial learning rate selected from  $\{5 \times 10^{-4}, 10^{-4}, 5 \times 10^{-5}\}$ . The training process was conducted for 10 epochs.

We adopted Mean Squared Error (MSE) and Mean Absolute Error (MAE) as our primary evaluation metrics. All baseline methods were evaluated using their respective official implementations to ensure a fair comparison. The entire framework was implemented in PyTorch and executed on a single NVIDIA A100 GPU.

## C. Full Results

Due to space limitations, the complete tables for the full results are provided in Appendix I. Experiments in the in-domain setting are shown in Table 8, while experiments in the cross-domain setting are presented in Table 9.

<sup>1</sup><https://github.com/blacksnail1789521/LLM4TS>

<sup>2</sup><https://github.com/KimMeen/Time-LLM>

<sup>3</sup><https://github.com/UNITES-Lab/FlowTS>

<sup>4</sup><https://github.com/zjt-gpu/CDPM>

<sup>5</sup><https://github.com/ermongroup/CSDI>

<sup>6</sup><https://github.com/Melmaphothe/TimeDART>

<sup>7</sup><https://github.com/yuqinie98/PatchTST>

<sup>8</sup><https://github.com/thuml/Autoformer>

## D. Ablation Study Full Results

### D.1. Encoder-Decoder Variants

As shown in Table 10, to validate the architectural design of our framework, we performed a comparative analysis between the complete encoder-decoder model and its two primary variants: Encoder-only and Decoder-only architectures, implemented with varying model sizes (0.6B and 1.7B). As presented in the ablation results, the full architecture yields superior forecasting accuracy across most benchmark datasets. The Decoder-only variants exhibit significant performance degradation, particularly on datasets with complex temporal patterns such as Health and Wind. This substantial drop in performance confirms that the bidirectional encoder is essential for capturing deep semantic representations and historical context, which are critical for effective time series forecasting. Crucially, our analysis reveals that the performance advantage of our proposed architecture is not merely a result of increased parameter count. Experiments prove that our full model consistently outperforms the Encoder-only variant, even when the latter is scaled to a significantly larger 1.7B backbone. This demonstrates that the structural synergy between bidirectional contextual understanding and causal generative refinement is the primary driver of our model’s effectiveness, offering consistent improvements.

### D.2. Ablation on AR-Flow

As shown in Table 11, to investigate the individual contributions of the two core generative components, we conducted a granular ablation study across all ten benchmarks by comparing the full framework with three restricted variants: w/o AR, which removes the bidirectional encoding and causal generation backbone; w/o Flow, which replaces the continuous flow-matching process with a deterministic output; and w/o AR-Flow, representing a baseline without either advancement. As shown in the ablation results, the full model consistently achieves superior precision, while the removal of either module leads to a noticeable performance decay across varying horizons. Specifically, the w/o AR variant exhibits a marked increase in both MSE and MAE, confirming that the LLM-based semantic reasoning and structural prior are fundamental for capturing complex, long-range temporal dependencies. Simultaneously, the w/o Flow variant yields inferior results compared to the full model, validating that the continuous flow-matching module is essential for effectively modeling the stochasticity and fine-grained dynamics in continuous-valued time series. The significant degradation observed in the w/o AR-Flow variant further underscores that the synergy between discrete semantic coupling and linearized continuous generation is the primary driver of our model’s superior forecasting stability.

### D.3. Ablation on Context Features

As shown in Table 12, to evaluate the specific contributions of various textual context components, we conducted a comprehensive ablation study across ten benchmarks by selectively removing domain knowledge, task instruction, and statistics information. As illustrated in the results, the full text-conditioned framework consistently achieves the best performance across all datasets and prediction horizons. Specifically, removing the entire textual input (w/o Text) leads to a universal degradation in forecasting precision, confirming that semantic context provides essential guidance for the generative process. Among the individual sub-components, the exclusion of statistics information (w/o Statistics) frequently results in a more pronounced increase in error compared to omitting domain features or instructions, as seen in datasets like Energy and Exchange. This suggests that explicit statistical metadata—such as mean and variance—is critical for the model to effectively align its generative distribution with the global data scale. Furthermore, the performance drop observed in the w/o Domain and w/o Instruction variants validates that high-level task descriptions and domain-specific knowledge further refine the model’s understanding capability, enabling more accurate capture of diverse temporal patterns. These results empirically verify that a multi-faceted semantic conditioning strategy is vital for high-precision time series forecasting.

## E. Comparison with Generative Models

As shown in Table 13, to verify the architectural advantages of our framework, we conducted a comprehensive comparison against two mainstream generative paradigms: vanilla flow-matching and diffusion models. As evidenced by the results across ten diverse benchmarks, our method consistently secures superior forecasting performance across all prediction horizons. Specifically, our model achieves a marked reduction in error metrics compared to Diffusion-based approaches, which often suffer from error accumulation during iterative denoising steps. Furthermore, our approach outperforms standard Flow-matching baselines by a significant margin, particularly on datasets with high volatility. This performance gap highlights the efficacy of our modeling objective, which explicitly targets a linearized generative path, thereby stabilizing

the generation process and effectively bridging high-level semantic understanding with continuous probabilistic modeling. As shown in Table 14, complementing this comparative analysis, we further examined the computational efficiency and stability of our generative process through an ablation study on the number of function evaluations (NFE). While traditional generative models typically require multiple sampling steps to ensure output fidelity, our results demonstrate that our framework achieves optimal or near-optimal forecasting accuracy with just a single evaluation step. Increasing the sampling steps to two or three yields only marginal performance gains in specific cases, while the one-step inference remains highly accurate across all datasets. This finding empirically confirms the straightness of the learned flow trajectories, proving that our linearized coupling strategy enables rapid, high-precision inference without the latency and computational overhead inherent in multi-step iterative solvers.

## F. Hyperparameter Sensitivity

### F.1. Patch Size

As shown in Table 16, to investigate the impact of local temporal granularity on forecasting performance, we conducted a sensitivity analysis by varying the patch size within the range of 2, 4, 6, 8, 10. As illustrated in the results, our model demonstrates varying degrees of sensitivity to this hyperparameter across different datasets, with intermediate patch sizes of 4 and 6 generally yielding the optimal balance between local detail and global structure. For instance, datasets such as ETTTh1, and Energy achieve their lowest errors with these settings. However, distinct patterns emerge for specific domains; the Environment and Exchange datasets favor a smaller patch size of 2, suggesting that these time series benefit from a higher-resolution tokenization to capture rapid, fine-grained fluctuations. Conversely, adopting an excessively large patch size (e.g., 10) consistently leads to performance degradation, most notably in the Health benchmark where the error significantly increases compared to the optimal setting. This deterioration likely stems from the smoothing effect of large patches, which obscures critical short-term dynamics required for accurate generation. Similarly, while small patches benefit specific domains, they prove suboptimal for complex systems like Health and Wind, where insufficient semantic context per token hampers the model’s understanding capabilities. These findings confirm that selecting an appropriate patch size is essential for effectively tokenizing continuous time series into semantically meaningful units.

### F.2. Noise Scheduler Analysis

As shown in Table 15, to investigate the impact of different noise scheduler strategies on forecasting performance, we conducted a comparative analysis between the linear scheduler and the cosine scheduler across ten real-world benchmarks. As illustrated in the results, the linear scheduler consistently yields superior results in terms of both MSE and MAE across almost all datasets. The superiority of the linear scheduler can be attributed to its uniform discretization, which perfectly aligns with our average velocity modeling objective that implies a constant-speed generative trajectory. Unlike the cosine scheduler, which introduces unnecessary temporal curvature, the linear scheduler ensures a straighter mapping that is more suitable for our one-step generation modeling, enabling precise inference in a single step without compromising accuracy. Consequently, we adopt the linear noise scheduler as our default configuration to maintain optimal forecasting precision.

## G. Analysis Experiment

### G.1. LLM Backbone

As shown in Table 17, to assess the impact of backbone architecture and parameter scale on forecasting fidelity, we conducted a comparative analysis between a vanilla Transformer and the Qwen LLM family across varying scales of 0.6B, 1.7B, and 4B. As evidenced in the results, all LLM-based variants significantly outperform the vanilla transformer across all benchmarks. This performance leap is primarily attributed to the superior representational capacity of LLMs and their ability to integrate contextual conditions, which provide a strong semantic understanding for conditioning the generation process. Within the Qwen family, while the Qwen3-4B model generally yields the lowest error metrics, the performance gap between the 4B model and the smaller 0.6B and 1.7B variants is often marginal. For instance, on datasets such as Exchange and ETTm1, the 0.6B model achieves results comparable to its larger counterparts. These findings suggest that for time series forecasting, the architectural advantages of a pre-trained LLM are effectively realized even at a compact scale. Consequently, balancing computational overhead, training latency, and predictive accuracy, we select Qwen3-0.6B as our default backbone, as it delivers performance approaching state-of-the-art levels with significantly higher inference efficiency.

## G.2. Extended-Length Look-back Window

As shown in Table 18, our framework is designed to support variable-length look-back windows without structural modifications. To validate this capability and evaluate the ability of the model to leverage long-term historical context, we investigated the impact of extending the look-back window size  $L$  from 96 to 192 and 336 across all ten benchmarks. The empirical results demonstrate that increasing the look-back window leads to progressive improvements in forecasting accuracy. Notably, on datasets with rich temporal dependencies like ETTh1 and Energy, extending the history from 96 to 336 steps results in a stable reduction in both MSE and MAE across all prediction horizons. This trend confirms that our model effectively utilizes the extended context to capture complex, long-range dependencies. The stable performance at  $L = 336$  further indicates that our hybrid generative architecture successfully aligns global historical patterns with local stochastic dynamics, maintaining high-precision trajectories even when processing significantly longer input sequences.

## H. Visualization

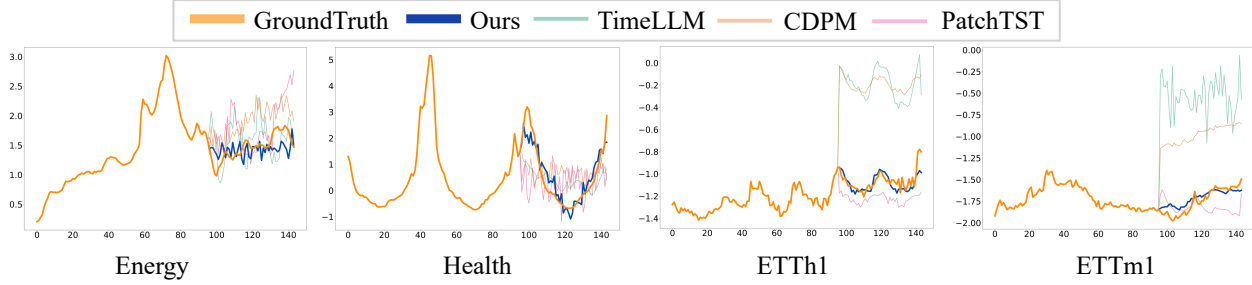


Figure 7. Comparison of forecasting results on Energy, Health, ETTh1, and ETThm1 datasets. We visualize the predicted trajectories of our method against the ground truth and leading baselines (Time-LLM, CDPM, and PatchTST).

To provide a qualitative assessment of forecasting fidelity, we visualize the predicted trajectories of our framework alongside the ground truth and competitive baselines, including Time-LLM, CDPM, and PatchTST. As illustrated in Figure 7, our model consistently generates future sequences that align most closely with the ground truth across diverse datasets such as Energy, Health, and the ETT series. Specifically, in datasets characterized by high volatility and complex seasonal patterns like Health, our model effectively captures the underlying stochastic dynamics without the severe over-smoothing or spurious fluctuations observed in baseline methods. Furthermore, for the ETTh1 and ETThm1 benchmarks, while competing methods often exhibit significant distributional shifts or phase delays, our approach maintains a stable and precise trend. This demonstrates the capability of our hybrid generative framework to bridge global semantic understanding with local continuous refinement. These visualized results empirically confirm that our model not only achieves superior numerical performance but also produces reliable and physically meaningful forecasts for real-world time series applications.

## I. Detailed Tables

This section provides the full experimental results for all evaluated benchmarks to offer a more granular perspective on the performance of CoGenCast. These detailed tables present the comprehensive forecasting metrics, including Mean Squared Error (MSE) and Mean Absolute Error (MAE), across various datasets and prediction horizons. Furthermore, this section includes complete results from our ablation studies, exhaustive comparisons with generative models, and systematic sensitivity analyses of key hyperparameters. Additional extended experimental analyses are also provided to further demonstrate the effectiveness and scalability of our proposed framework across diverse scenarios.

Table 8. Full results of time series forecasting across all benchmark datasets. We provide a detailed comparison between our proposed framework and competitive baselines, including LLM-based, generative-based, and transformer-based methods, evaluated on look-back window  $L = 336$  and four predicted windows  $H \in \{12, 24, 36, 48\}$ . The best results are in **bold** and the second best are underlined.

METHODS	OURS	LLM-BASED				GENERATIVE-BASED						TRANSFORMER-BASED							
		LLM4TS		Time-LLM		FlowTS	CDPM	CSDI	TimeDART		PatchTST		Autoformer						
METRICS		MSE	MAE	MSE	MAE	MSE	MAE	MSE	MAE	MSE	MAE	MSE	MAE	MSE	MAE	MSE	MAE		
Energy	12	<b>0.140</b>	<b>0.273</b>	0.177	0.321	0.180	0.324	0.354	0.402	0.210	0.351	0.603	0.606	0.177	0.321	<u>0.175</u>	<u>0.320</u>	0.461	0.518
	24	<b>0.265</b>	<b>0.379</b>	0.293	0.405	0.291	0.404	0.392	0.448	0.349	0.427	0.642	0.623	<u>0.283</u>	<u>0.394</u>	0.288	0.398	0.484	0.528
	36	<b>0.327</b>	<b>0.428</b>	<u>0.340</u>	<u>0.442</u>	0.345	0.445	0.441	0.503	0.460	0.484	0.687	0.636	0.362	0.455	0.366	0.457	0.488	0.540
	48	<b>0.441</b>	0.499	<u>0.461</u>	<b>0.483</b>	0.482	0.521	0.485	0.539	0.473	0.524	0.744	0.669	0.469	0.513	0.479	0.522	0.591	0.581
ETTh1	12	<b>0.290</b>	<b>0.343</b>	0.314	0.365	0.318	0.364	0.311	<u>0.352</u>	0.313	0.359	1.147	0.934	0.319	0.362	0.321	0.365	0.434	0.416
	24	<b>0.319</b>	<b>0.362</b>	0.330	0.375	0.387	0.406	0.356	0.389	0.337	<u>0.374</u>	1.238	0.966	0.343	0.376	0.352	0.382	0.481	0.470
	36	<b>0.344</b>	<b>0.377</b>	0.358	<u>0.385</u>	0.358	0.387	0.404	0.431	<u>0.356</u>	0.387	1.489	0.982	0.366	0.391	0.384	0.401	0.519	0.492
	48	<b>0.357</b>	<b>0.386</b>	<u>0.388</u>	<u>0.402</u>	0.393	0.408	0.453	0.480	0.392	0.410	1.546	0.953	0.389	0.405	0.411	0.413	0.544	0.498
ETTh2	12	0.121	<b>0.216</b>	0.135	0.236	0.146	0.249	0.168	0.261	0.145	0.248	0.568	0.526	<u>0.111</u>	0.226	<b>0.110</b>	<u>0.225</u>	0.172	0.283
	24	0.152	<b>0.243</b>	0.190	0.282	0.199	0.289	0.192	0.283	0.175	0.267	0.650	0.560	<u>0.133</u>	0.246	<b>0.129</b>	<b>0.243</b>	0.190	0.302
	36	0.172	<b>0.254</b>	0.221	0.302	0.232	0.309	0.249	0.318	0.222	0.300	0.601	0.534	<u>0.155</u>	0.263	<b>0.150</b>	<u>0.259</u>	0.197	0.308
	48	0.191	<b>0.272</b>	0.234	0.305	0.246	0.317	0.263	0.339	0.229	0.301	0.768	0.645	<u>0.179</u>	0.278	<b>0.178</b>	<u>0.276</u>	0.209	0.312
ETTm1	12	<b>0.140</b>	<b>0.232</b>	0.173	<u>0.262</u>	0.182	0.271	0.267	0.320	0.201	0.304	0.766	0.590	<u>0.159</u>	<u>0.262</u>	0.165	0.267	0.282	0.347
	24	<b>0.213</b>	<b>0.280</b>	0.248	0.312	0.323	0.365	0.305	0.351	0.309	0.351	0.881	0.638	<u>0.231</u>	<u>0.303</u>	0.236	0.308	0.337	0.391
	36	<b>0.255</b>	<b>0.306</b>	0.285	0.334	0.361	0.381	0.344	0.391	0.333	0.369	0.945	0.661	0.274	0.328	<u>0.271</u>	<u>0.327</u>	0.399	0.442
	48	<b>0.288</b>	<b>0.321</b>	0.307	0.346	0.349	0.377	0.392	0.434	0.365	0.382	0.998	0.703	<u>0.297</u>	<u>0.343</u>	0.301	0.345	0.483	0.549
ETTm2	12	<b>0.079</b>	<b>0.167</b>	0.115	0.227	0.109	0.218	0.149	0.256	0.144	0.252	0.721	0.567	<u>0.101</u>	<u>0.201</u>	0.102	0.203	0.218	0.347
	24	<b>0.102</b>	<b>0.194</b>	0.138	0.247	0.139	0.245	0.191	0.299	0.185	0.296	0.885	0.656	<u>0.113</u>	<u>0.225</u>	0.117	0.228	0.234	0.365
	36	<b>0.120</b>	<b>0.212</b>	0.156	0.262	0.153	0.256	0.216	0.326	0.210	0.321	0.993	0.731	<u>0.130</u>	<u>0.239</u>	0.134	0.241	0.246	0.372
	48	<b>0.134</b>	<b>0.226</b>	0.170	0.271	0.162	0.268	0.233	0.339	0.225	0.333	1.154	0.887	<u>0.146</u>	<u>0.261</u>	0.151	0.266	0.254	0.376
Environ.	12	<b>0.286</b>	<b>0.372</b>	0.302	0.388	0.298	0.386	<b>0.286</b>	<b>0.361</b>	0.319	0.428	1.023	0.845	0.295	0.389	0.292	0.387	0.346	0.436
	24	<b>0.295</b>	<b>0.378</b>	0.312	<u>0.393</u>	0.319	0.401	0.322	0.404	0.330	0.397	1.171	0.873	0.307	0.395	<u>0.302</u>	<u>0.393</u>	0.358	0.459
	36	<b>0.305</b>	<b>0.383</b>	0.321	<u>0.398</u>	0.325	0.403	0.369	0.447	0.349	0.444	1.304	0.890	0.321	0.404	<u>0.315</u>	0.400	0.379	0.475
	48	<b>0.316</b>	<b>0.390</b>	0.330	<u>0.401</u>	0.337	0.411	0.419	0.488	0.338	0.407	1.499	0.923	0.333	0.409	<u>0.327</u>	0.407	0.381	0.473
Exchange	12	<b>0.015</b>	<b>0.079</b>	0.023	0.106	0.019	0.096	0.041	0.138	0.029	0.124	0.514	0.553	<u>0.017</u>	0.094	0.018	<u>0.093</u>	0.057	0.173
	24	<b>0.026</b>	<b>0.110</b>	0.032	0.125	0.030	0.121	0.054	0.169	0.034	0.131	0.557	0.582	0.030	0.119	<u>0.028</u>	<u>0.118</u>	0.084	0.212
	36	<b>0.037</b>	<b>0.132</b>	0.041	0.142	<u>0.039</u>	<u>0.141</u>	0.069	0.201	0.057	0.173	0.673	0.698	0.040	0.142	<u>0.039</u>	0.143	0.089	0.219
	48	<b>0.046</b>	<b>0.150</b>	0.051	0.158	0.053	0.163	0.080	0.232	0.065	0.183	0.769	0.791	<u>0.048</u>	0.153	<u>0.048</u>	0.155	0.117	0.250
Health	12	<b>1.056</b>	<b>0.697</b>	1.351	0.809	1.311	0.781	1.482	0.824	1.298	0.788	2.046	1.094	<u>1.119</u>	<u>0.736</u>	1.224	0.750	1.737	0.987
	24	<b>1.500</b>	<b>0.820</b>	1.570	0.875	1.602	0.865	1.621	0.901	1.569	0.870	2.130	1.200	<u>1.544</u>	<u>0.851</u>	1.556	0.857	1.809	1.014
	36	<b>1.583</b>	<b>0.852</b>	1.878	1.001	1.713	0.901	1.815	0.985	1.682	0.907	2.247	1.311	1.639	0.892	<u>1.636</u>	<u>0.889</u>	1.845	1.018
	48	<b>1.638</b>	<b>0.879</b>	1.918	1.007	1.818	0.999	2.026	1.062	1.815	1.022	2.449	1.478	<u>1.737</u>	<u>0.927</u>	1.743	0.931	1.919	1.051
Wind	12	<b>0.269</b>	<b>0.263</b>	0.351	0.355	0.281	0.289	0.521	0.424	0.350	0.342	0.790	0.603	0.278	0.289	<u>0.274</u>	<u>0.286</u>	0.647	0.532
	24	<b>0.479</b>	<b>0.399</b>	0.536	0.457	0.486	0.417	0.603	0.467	0.533	0.444	0.891	0.644	0.486	0.417	<u>0.484</u>	<u>0.415</u>	0.765	0.584
	36	<b>0.637</b>	<b>0.488</b>	0.675	0.526	0.655	0.512	0.692	0.518	0.667	0.514	0.946	0.665	0.652	0.508	<u>0.649</u>	<u>0.504</u>	0.857	0.618
	48	<b>0.741</b>	<b>0.549</b>	0.801	0.599	0.751	0.559	0.788	0.579	0.782	0.571	1.003	0.689	0.750	0.559	<u>0.749</u>	<u>0.557</u>	0.1051	0.701
Solar	12	<b>0.115</b>	<b>0.206</b>	0.124	0.222	0.122	<u>0.211</u>	0.295	0.341	0.237	0.340	0.796	0.705	0.123	0.213	<u>0.121</u>	0.212	0.407	0.507
	24	<b>0.216</b>	<b>0.285</b>	0.236	0.309	0.228	0.298	0.344	0.396	0.352	0.414	0.873	0.747	0.228	0.297	<u>0.223</u>	<u>0.294</u>	0.725	0.671
	36	<b>0.288</b>	<b>0.338</b>	0.293	0.348	<u>0.289</u>	<u>0.339</u>	0.398	0.453	0.407	0.451	1.015	0.809	0.301	0.351	0.297	0.347	0.594	0.586
	48	<b>0.276</b>	<b>0.328</b>	0.301	0.349	0.294	0.346	0.439	0.498	0.405	0.436	1.174	0.883	0.291	0.343	<u>0.286</u>	<u>0.339</u>	0.917	0.741

Table 9. Full results of in-domain and cross-domain training across all benchmark datasets. Results are reported in MSE and MAE for each predicted windows  $H \in \{12, 24, 36, 48\}$ . The best results are in **bold**.

HORIZON	METRICS	ENERGY		ETTH1		ETTH2		ETTM1		ETTM2		ENVIRON.		EXCHANGE		HEALTH		WIND		SOLAR	
		In	Cross	In	Cross	In	Cross	In	Cross	In	Cross	In	Cross	In	Cross	In	Cross	In	Cross	In	Cross
12	MSE	0.140	<b>0.137</b>	0.290	<b>0.286</b>	0.121	<b>0.119</b>	0.140	<b>0.138</b>	0.079	<b>0.078</b>	0.286	<b>0.282</b>	<b>0.015</b>	<b>0.015</b>	1.056	<b>1.049</b>	0.269	<b>0.267</b>	0.115	<b>0.114</b>
	MAE	0.273	<b>0.271</b>	0.343	<b>0.341</b>	0.216	<b>0.215</b>	0.232	<b>0.230</b>	0.167	<b>0.166</b>	0.372	<b>0.368</b>	<b>0.079</b>	<b>0.079</b>	0.697	<b>0.692</b>	0.263	<b>0.262</b>	<b>0.206</b>	<b>0.206</b>
24	MSE	0.265	<b>0.262</b>	0.319	<b>0.315</b>	0.152	<b>0.151</b>	0.213	<b>0.210</b>	0.102	<b>0.100</b>	0.295	<b>0.291</b>	0.026	<b>0.025</b>	1.500	<b>1.487</b>	0.479	<b>0.475</b>	0.216	<b>0.214</b>
	MAE	0.379	<b>0.375</b>	0.362	<b>0.359</b>	0.243	<b>0.242</b>	0.280	<b>0.278</b>	0.194	<b>0.191</b>	0.378	<b>0.375</b>	<b>0.110</b>	<b>0.110</b>	0.820	<b>0.812</b>	0.399	<b>0.397</b>	0.285	<b>0.283</b>
36	MSE	0.327	<b>0.323</b>	0.344	<b>0.341</b>	0.172	<b>0.170</b>	0.255	<b>0.252</b>	0.120	<b>0.116</b>	0.305	<b>0.302</b>	0.037	<b>0.036</b>	1.583	<b>1.539</b>	0.637	<b>0.629</b>	0.288	<b>0.284</b>
	MAE	0.428	<b>0.424</b>	0.377	<b>0.373</b>	0.254	<b>0.251</b>	0.306	<b>0.304</b>	0.212	<b>0.209</b>	0.383	<b>0.379</b>	0.132	<b>0.130</b>	0.852	<b>0.846</b>	0.488	<b>0.483</b>	0.338	<b>0.335</b>
48	MSE	0.441	<b>0.436</b>	0.357	<b>0.352</b>	0.191	<b>0.189</b>	0.288	<b>0.285</b>	0.134	<b>0.131</b>	0.316	<b>0.311</b>	0.046	<b>0.044</b>	1.638	<b>1.614</b>	0.741	<b>0.736</b>	0.276	<b>0.273</b>
	MAE	0.499	<b>0.491</b>	0.386	<b>0.389</b>	0.272	<b>0.271</b>	0.321	<b>0.319</b>	0.226	<b>0.222</b>	0.390	<b>0.386</b>	0.150	<b>0.147</b>	0.879	<b>0.865</b>	0.549	<b>0.550</b>	0.328	<b>0.325</b>

Table 10. Full results of the ablation study on the encoder-decoder architecture. We compare our framework against encoder-only and decoder-only variants equipped with Qwen3-0.6B and Qwen3-1.7B backbones across all benchmark datasets. The best results are in **bold**.

METRICS	METHODS	OURS		ENCODER-ONLY				DECODER-ONLY				
		MSE	MAE	Qwen3-0.6B		Qwen3-1.7B		MSE	MAE	MSE	MAE	
				MSE	MAE	MSE	MAE					
Energy		12	<b>0.140</b>	<b>0.273</b>	0.180	0.331	0.179	0.331	0.510	0.537	0.479	0.519
		24	<b>0.265</b>	<b>0.379</b>	0.293	0.403	0.292	0.402	0.810	0.715	0.762	0.688
		36	<b>0.327</b>	<b>0.428</b>	0.355	0.447	0.354	0.446	1.166	0.831	1.090	0.798
		48	<b>0.441</b>	<b>0.499</b>	0.495	0.540	0.494	0.539	1.324	0.884	1.247	0.854
ETTh1		12	<b>0.290</b>	<b>0.343</b>	0.307	0.353	0.302	0.354	0.945	0.655	0.817	0.626
		24	<b>0.319</b>	<b>0.362</b>	0.346	0.391	0.338	0.376	1.047	0.691	0.899	0.663
		36	<b>0.344</b>	<b>0.377</b>	0.356	0.388	0.352	0.390	1.134	0.720	0.967	0.688
		48	<b>0.357</b>	<b>0.386</b>	0.372	0.398	0.368	0.401	1.213	0.745	1.006	0.707
ETTh2		12	<b>0.121</b>	<b>0.216</b>	0.146	0.239	0.129	0.225	0.386	0.404	0.352	0.389
		24	<b>0.152</b>	<b>0.243</b>	0.169	0.257	0.165	0.256	0.482	0.456	0.440	0.438
		36	<b>0.172</b>	<b>0.254</b>	0.185	0.266	0.184	0.265	0.540	0.474	0.493	0.456
		48	<b>0.191</b>	<b>0.272</b>	0.206	0.284	0.206	0.286	0.600	0.510	0.547	0.489
ETTm1		12	<b>0.140</b>	<b>0.232</b>	0.159	0.256	0.154	0.251	0.760	0.562	0.612	0.484
		24	<b>0.213</b>	<b>0.280</b>	0.240	0.309	0.234	0.305	1.045	0.650	0.934	0.586
		36	<b>0.255</b>	<b>0.306</b>	0.273	0.332	0.268	0.331	1.270	0.709	1.116	0.638
		48	<b>0.288</b>	<b>0.321</b>	0.309	0.351	0.304	0.349	1.506	0.762	1.262	0.672
ETTm2		12	<b>0.079</b>	<b>0.167</b>	0.091	0.184	0.086	0.175	0.338	0.408	0.289	0.359
		24	<b>0.102</b>	<b>0.194</b>	0.119	0.216	0.114	0.206	0.439	0.476	0.375	0.420
		36	<b>0.120</b>	<b>0.212</b>	0.138	0.234	0.131	0.223	0.514	0.518	0.439	0.456
		48	<b>0.134</b>	<b>0.226</b>	0.156	0.250	0.149	0.240	0.577	0.554	0.493	0.489
Environ.		12	<b>0.286</b>	<b>0.372</b>	0.298	0.388	0.296	0.393	0.576	0.565	0.536	0.539
		24	<b>0.295</b>	<b>0.378</b>	0.303	0.402	0.302	0.401	0.590	0.568	0.552	0.548
		36	<b>0.305</b>	<b>0.383</b>	0.317	0.409	0.315	0.404	0.613	0.576	0.574	0.555
		48	<b>0.316</b>	<b>0.390</b>	0.333	0.415	0.329	0.414	0.629	0.586	0.589	0.567
Exchange		12	<b>0.015</b>	<b>0.079</b>	0.020	0.098	0.018	0.092	0.049	0.152	0.081	0.171
		24	<b>0.026</b>	<b>0.110</b>	0.031	0.124	0.030	0.126	0.100	0.210	0.143	0.222
		36	<b>0.037</b>	<b>0.132</b>	0.040	0.142	0.039	0.141	0.198	0.280	0.201	0.265
		48	<b>0.046</b>	<b>0.150</b>	0.052	0.163	0.051	0.157	0.406	0.377	0.252	0.303
Health		12	<b>1.056</b>	<b>0.697</b>	1.165	0.714	1.155	0.740	3.891	1.528	2.622	1.193
		24	<b>1.500</b>	<b>0.820</b>	1.624	0.881	1.612	0.873	3.847	1.519	3.726	1.406
		36	<b>1.583</b>	<b>0.852</b>	1.715	0.893	1.702	0.905	4.115	1.572	3.931	1.459
		48	<b>1.638</b>	<b>0.879</b>	1.803	0.945	1.855	0.935	4.243	1.587	4.069	1.507
Wind		12	<b>0.269</b>	<b>0.263</b>	0.278	0.297	0.275	0.279	0.842	0.567	0.894	0.475
		24	<b>0.479</b>	<b>0.399</b>	0.495	0.432	0.491	0.426	1.534	0.759	1.594	0.723
		36	<b>0.637</b>	<b>0.488</b>	0.653	0.514	0.649	0.518	2.333	0.922	2.118	0.883
		48	<b>0.741</b>	<b>0.549</b>	0.760	0.568	0.756	0.585	3.331	1.082	2.467	1.002
Solar		12	<b>0.115</b>	<b>0.206</b>	0.124	0.224	0.122	0.214	0.768	0.511	0.136	0.223
		24	<b>0.216</b>	<b>0.285</b>	0.230	0.302	0.227	0.299	0.877	0.602	0.258	0.311
		36	<b>0.288</b>	<b>0.338</b>	0.300	0.350	0.297	0.341	0.985	0.764	0.341	0.367
		48	<b>0.276</b>	<b>0.328</b>	0.292	0.345	0.288	0.354	0.915	0.699	0.329	0.358

Table 11. Full results of the ablation study on the generative components. We compare the forecasting performance of our full framework against variants without the autoregressive mechanism (w/o AR), without the flow-matching mechanism (w/o Flow), and without both components (w/o AR-Flow) across all benchmark datasets. The best results are in **bold**.

METHODS METRICS		OURS		w/o AR		w/o FLOW		w/o AR-Flow	
		MSE	MAE	MSE	MAE	MSE	MAE	MSE	MAE
Energy	12	<b>0.140</b>	<b>0.273</b>	0.184	0.326	0.178	0.318	0.187	0.331
	24	<b>0.265</b>	<b>0.379</b>	0.300	0.401	0.296	0.398	0.305	0.402
	36	<b>0.327</b>	<b>0.428</b>	0.366	0.445	0.360	0.442	0.360	0.441
	48	0.441	0.499	0.506	0.536	0.500	0.530	<b>0.378</b>	<b>0.452</b>
ETTh1	12	<b>0.290</b>	<b>0.343</b>	0.323	0.375	0.316	0.368	0.329	0.377
	24	<b>0.319</b>	<b>0.362</b>	0.358	0.398	0.350	0.390	0.364	0.401
	36	<b>0.344</b>	<b>0.377</b>	0.383	0.412	0.375	0.405	0.390	0.415
	48	<b>0.357</b>	<b>0.386</b>	0.400	0.423	0.391	0.416	0.407	0.426
ETTh2	12	<b>0.121</b>	<b>0.216</b>	0.141	0.234	0.136	0.231	0.145	0.239
	24	<b>0.152</b>	<b>0.243</b>	0.179	0.265	0.173	0.262	0.184	0.270
	36	<b>0.172</b>	<b>0.254</b>	0.200	0.275	0.194	0.271	0.205	0.281
	48	<b>0.191</b>	<b>0.272</b>	0.224	0.298	0.217	0.292	0.230	0.302
ETTm1	12	<b>0.140</b>	<b>0.232</b>	0.160	0.262	0.156	0.257	0.163	0.265
	24	<b>0.213</b>	<b>0.280</b>	0.245	0.318	0.240	0.312	0.250	0.322
	36	<b>0.255</b>	<b>0.306</b>	0.291	0.345	0.285	0.339	0.297	0.349
	48	<b>0.288</b>	<b>0.321</b>	0.331	0.364	0.324	0.358	0.338	0.369
ETTm2	12	<b>0.079</b>	<b>0.167</b>	0.096	0.190	0.093	0.187	0.101	0.195
	24	<b>0.102</b>	<b>0.194</b>	0.127	0.223	0.122	0.220	0.133	0.228
	36	<b>0.120</b>	<b>0.212</b>	0.147	0.242	0.141	0.238	0.155	0.247
	48	<b>0.134</b>	<b>0.226</b>	0.166	0.261	0.160	0.255	0.175	0.266
Environ.	12	<b>0.286</b>	<b>0.372</b>	0.325	0.395	0.320	0.389	0.332	0.399
	24	<b>0.295</b>	<b>0.378</b>	0.331	0.408	0.326	0.403	0.338	0.413
	36	<b>0.305</b>	<b>0.383</b>	0.346	0.415	0.341	0.410	0.353	0.420
	48	<b>0.316</b>	<b>0.390</b>	0.362	0.422	0.354	0.415	0.367	0.425
Exchange	12	<b>0.015</b>	<b>0.079</b>	0.028	0.094	0.025	0.090	0.030	0.096
	24	<b>0.026</b>	<b>0.110</b>	0.052	0.134	0.046	0.128	0.055	0.137
	36	<b>0.037</b>	<b>0.132</b>	0.072	0.158	0.063	0.151	0.076	0.162
	48	<b>0.046</b>	<b>0.150</b>	0.092	0.182	0.081	0.174	0.097	0.186
Health	12	<b>1.056</b>	<b>0.697</b>	1.264	0.745	1.221	0.740	1.296	0.754
	24	<b>1.500</b>	<b>0.820</b>	1.777	0.879	1.737	0.873	1.843	0.889
	36	<b>1.583</b>	<b>0.852</b>	1.973	0.911	1.831	0.905	1.943	0.921
	48	<b>1.638</b>	<b>0.879</b>	1.940	0.942	1.896	0.935	2.013	0.953
Wind	12	<b>0.269</b>	<b>0.263</b>	0.340	0.311	0.308	0.297	0.359	0.322
	24	<b>0.479</b>	<b>0.399</b>	0.608	0.474	0.552	0.454	0.642	0.491
	36	<b>0.637</b>	<b>0.488</b>	0.806	0.577	0.731	0.553	0.851	0.599
	48	<b>0.741</b>	<b>0.549</b>	0.938	0.642	0.852	0.624	0.992	0.676
Solar	12	<b>0.115</b>	<b>0.206</b>	0.143	0.232	0.136	0.223	0.149	0.239
	24	<b>0.216</b>	<b>0.285</b>	0.270	0.323	0.258	0.311	0.282	0.333
	36	<b>0.288</b>	<b>0.338</b>	0.358	0.381	0.341	0.367	0.374	0.393
	48	<b>0.276</b>	<b>0.328</b>	0.345	0.372	0.329	0.358	0.360	0.383

Table 12. Full results of the ablation study on context features. We compare the forecasting performance of our full framework against variants without domain knowledge (w/o Domain), task instruction (w/o Instruction), statistics information (w/o Statistics), and the entire textual input (w/o Text) across all benchmark datasets. The best results are in **bold**.

METHODS METRICS	OURS		W/O DOMAIN		W/O INSTRUCTION		W/O STATISTICS		W/O TEXT		
	MSE	MAE	MSE	MAE	MSE	MAE	MSE	MAE	MSE	MAE	
Energy	12	<b>0.140</b>	<b>0.273</b>	0.145	0.282	0.143	0.277	0.151	0.292	0.156	0.305
	24	<b>0.265</b>	<b>0.379</b>	0.268	0.381	0.267	0.380	0.273	0.383	0.277	0.386
	36	<b>0.327</b>	<b>0.428</b>	0.334	0.433	0.331	0.430	0.344	0.438	0.351	0.444
	48	<b>0.441</b>	<b>0.499</b>	0.445	0.501	0.443	0.500	0.452	0.502	0.457	0.504
ETTh1	12	<b>0.290</b>	<b>0.343</b>	0.304	0.345	0.308	0.348	0.304	0.354	0.310	0.355
	24	<b>0.319</b>	<b>0.362</b>	0.330	0.364	0.333	0.366	0.330	0.370	0.335	0.371
	36	<b>0.344</b>	<b>0.377</b>	0.354	0.379	0.357	0.381	0.354	0.386	0.358	0.387
	48	<b>0.357</b>	<b>0.386</b>	0.368	0.388	0.370	0.390	0.368	0.395	0.372	0.396
ETTh2	12	<b>0.121</b>	<b>0.216</b>	0.123	0.218	0.123	0.218	0.128	0.223	0.130	0.225
	24	<b>0.152</b>	<b>0.243</b>	0.154	0.245	0.155	0.246	0.161	0.251	0.164	0.253
	36	<b>0.172</b>	<b>0.254</b>	0.174	0.256	0.175	0.257	0.182	0.262	0.185	0.264
	48	<b>0.191</b>	<b>0.272</b>	0.193	0.274	0.195	0.275	0.202	0.281	0.205	0.283
ETTm1	12	<b>0.140</b>	<b>0.232</b>	0.144	0.245	0.145	0.246	0.154	0.254	0.159	0.258
	24	<b>0.213</b>	<b>0.280</b>	0.216	0.282	0.217	0.283	0.224	0.291	0.228	0.295
	36	<b>0.255</b>	<b>0.306</b>	0.257	0.309	0.258	0.311	0.264	0.319	0.267	0.321
	48	<b>0.288</b>	<b>0.321</b>	0.290	0.323	0.291	0.325	0.297	0.332	0.300	0.335
ETTm2	12	<b>0.079</b>	<b>0.167</b>	0.081	0.169	0.080	0.168	0.085	0.175	0.086	0.177
	24	<b>0.102</b>	<b>0.194</b>	0.105	0.196	0.103	0.195	0.110	0.203	0.112	0.206
	36	<b>0.120</b>	<b>0.212</b>	0.124	0.214	0.121	0.213	0.129	0.222	0.131	0.225
	48	<b>0.134</b>	<b>0.226</b>	0.138	0.229	0.136	0.227	0.144	0.236	0.147	0.240
Environ.	12	<b>0.286</b>	<b>0.372</b>	0.288	0.373	0.287	0.373	0.290	0.375	0.291	0.376
	24	<b>0.295</b>	<b>0.378</b>	0.297	0.379	0.296	0.379	0.299	0.380	0.300	0.381
	36	<b>0.305</b>	<b>0.383</b>	0.308	0.384	0.307	0.384	0.312	0.386	0.313	0.387
	48	<b>0.316</b>	<b>0.390</b>	0.319	0.392	0.318	0.392	0.323	0.395	0.324	0.396
Exchange	12	<b>0.015</b>	<b>0.079</b>	0.016	0.080	0.016	0.081	0.018	0.083	0.018	0.084
	24	<b>0.026</b>	<b>0.110</b>	0.027	0.111	0.027	0.112	0.029	0.115	0.029	0.116
	36	<b>0.037</b>	<b>0.132</b>	0.038	0.134	0.038	0.134	0.039	0.136	0.040	0.137
	48	<b>0.046</b>	<b>0.150</b>	0.047	0.153	0.047	0.153	0.050	0.158	0.051	0.160
Health	12	<b>1.056</b>	<b>0.697</b>	1.063	0.701	1.074	0.705	1.090	0.796	1.112	0.713
	24	<b>1.500</b>	<b>0.820</b>	1.504	0.824	1.511	0.827	1.521	0.931	1.534	0.834
	36	<b>1.583</b>	<b>0.852</b>	1.587	0.855	1.594	0.857	1.604	0.962	1.617	0.862
	48	<b>1.638</b>	<b>0.879</b>	1.645	0.881	1.657	0.883	1.673	0.990	1.696	0.887
Wind	12	<b>0.269</b>	<b>0.263</b>	0.272	0.267	0.271	0.265	0.275	0.280	0.277	0.288
	24	<b>0.479</b>	<b>0.399</b>	0.482	0.401	0.481	0.400	0.485	0.407	0.487	0.410
	36	<b>0.637</b>	<b>0.488</b>	0.641	0.490	0.640	0.489	0.646	0.495	0.650	0.498
	48	<b>0.741</b>	<b>0.549</b>	0.745	0.550	0.744	0.550	0.750	0.554	0.753	0.557
Solar	12	<b>0.115</b>	<b>0.206</b>	0.117	0.207	0.119	0.208	0.120	0.210	0.122	0.211
	24	<b>0.216</b>	<b>0.286</b>	0.219	0.288	0.222	0.290	0.224	0.293	0.226	0.295
	36	<b>0.288</b>	<b>0.338</b>	0.295	0.345	0.299	0.347	0.301	0.351	0.303	0.354
	48	<b>0.276</b>	<b>0.328</b>	0.286	0.336	0.290	0.338	0.292	0.342	0.283	0.335

Table 13. Full results of the comparative analysis among different generative methods. We compare our proposed framework with vanilla flow-matching and diffusion models across all benchmark datasets. The best results are in **bold**.

HORIZON METRICS		ENERGY			ETTH1			ETTH2			ETTM1			ETTM2			ENVIRON.			EXCHANGE			HEALTH			WIND			SOLAR		
		Ours	Flow	Diff																											
12	MSE	<b>0.140</b>	0.158	0.155	<b>0.290</b>	0.329	0.321	<b>0.121</b>	0.147	0.146	<b>0.140</b>	0.186	0.179	<b>0.079</b>	0.108	0.105	<b>0.286</b>	0.313	0.306	<b>0.015</b>	0.025	0.022	<b>1.056</b>	1.171	1.157	<b>0.269</b>	0.306	0.298	<b>0.115</b>	0.135	0.132
	MAE	<b>0.273</b>	0.289	0.286	<b>0.343</b>	0.373	0.368	<b>0.216</b>	0.239	0.236	<b>0.232</b>	0.279	0.272	<b>0.167</b>	0.199	0.196	<b>0.372</b>	0.390	0.386	<b>0.079</b>	0.088	0.085	<b>0.697</b>	0.724	0.710	<b>0.263</b>	0.296	0.289	<b>0.206</b>	0.221	0.219
24	MSE	<b>0.265</b>	0.300	0.294	<b>0.319</b>	0.362	0.354	<b>0.152</b>	0.185	0.183	<b>0.213</b>	0.283	0.272	<b>0.102</b>	0.140	0.136	<b>0.295</b>	0.323	0.316	<b>0.026</b>	0.043	0.039	<b>1.500</b>	1.663	1.644	<b>0.479</b>	0.545	0.530	<b>0.216</b>	0.255	0.249
	MAE	<b>0.379</b>	0.401	0.397	<b>0.362</b>	0.394	0.389	<b>0.243</b>	0.268	0.265	<b>0.280</b>	0.336	0.328	<b>0.194</b>	0.231	0.228	<b>0.378</b>	0.396	0.392	<b>0.110</b>	0.122	0.119	<b>0.820</b>	0.851	0.835	<b>0.399</b>	0.449	0.439	<b>0.286</b>	0.307	0.303
36	MSE	<b>0.327</b>	0.370	0.362	<b>0.344</b>	0.391	0.381	<b>0.172</b>	0.209	0.206	<b>0.255</b>	0.339	0.326	<b>0.120</b>	0.164	0.160	<b>0.305</b>	0.334	0.327	<b>0.037</b>	0.061	0.055	<b>1.583</b>	1.755	1.735	<b>0.637</b>	0.725	0.705	<b>0.288</b>	0.345	0.336
	MAE	<b>0.428</b>	0.453	0.448	<b>0.377</b>	0.410	0.405	<b>0.254</b>	0.281	0.277	<b>0.306</b>	0.368	0.359	<b>0.212</b>	0.253	0.249	<b>0.383</b>	0.401	0.397	<b>0.132</b>	0.147	0.142	<b>0.852</b>	0.885	0.868	<b>0.488</b>	0.549	0.537	<b>0.338</b>	0.368	0.364
48	MSE	<b>0.441</b>	0.499	0.489	<b>0.357</b>	0.406	0.396	<b>0.191</b>	0.231	0.229	<b>0.288</b>	0.383	0.368	<b>0.134</b>	0.184	0.179	<b>0.316</b>	0.346	0.339	<b>0.046</b>	0.076	0.068	<b>1.638</b>	1.816	1.795	<b>0.741</b>	0.843	0.820	<b>0.276</b>	0.335	0.327
	MAE	<b>0.499</b>	0.528	0.522	<b>0.386</b>	0.420	0.414	<b>0.272</b>	0.300	0.297	<b>0.321</b>	0.386	0.377	<b>0.226</b>	0.269	0.266	<b>0.390</b>	0.409	0.405	<b>0.150</b>	0.167	0.162	<b>0.879</b>	0.913	0.895	<b>0.549</b>	0.618	0.604	<b>0.328</b>	0.359	0.355

Table 14. Full results of the efficiency-performance trade-off analysis regarding the number of function evaluations (NFE). We compare the forecasting performance using 1, 2, and 3 sampling steps across all benchmark datasets. The best results are in **bold**.

HORIZON METRICS		ENERGY			ETTH1			ETTH2			ETTM1			ETTM2			ENVIRON.			EXCHANGE			HEALTH			WIND			SOLAR		
		1	2	3	1	2	3	1	2	3	1	2	3	1	2	3	1	2	3	1	2	3	1	2	3	1	2	3			
12	MSE	0.140	<b>0.139</b>	0.147	0.290	<b>0.288</b>	0.306	0.121	<b>0.119</b>	0.123	0.140	<b>0.139</b>	0.143	0.079	<b>0.077</b>	0.082	<b>0.286</b>	<b>0.286</b>	0.287	<b>0.015</b>	<b>0.015</b>	0.016	1.056	<b>1.051</b>	1.076	0.269	<b>0.265</b>	0.274	0.115	<b>0.114</b>	0.118
	MAE	0.273	<b>0.272</b>	0.277	0.343	<b>0.341</b>	0.356	0.216	<b>0.214</b>	0.218	0.232	<b>0.230</b>	0.237	0.167	<b>0.166</b>	0.171	0.372	<b>0.370</b>	0.373	0.079	<b>0.078</b>	0.081	0.697	0.694	0.703	0.263	<b>0.259</b>	0.268	0.206	<b>0.203</b>	0.209
24	MSE	0.265	<b>0.263</b>	0.279	0.319	<b>0.317</b>	0.337	0.152	<b>0.150</b>	0.154	0.213	<b>0.211</b>	0.217	0.102	<b>0.099</b>	0.106	<b>0.295</b>	<b>0.295</b>	0.296	0.026	<b>0.025</b>	0.027	1.500	<b>1.492</b>	1.528	0.479	<b>0.472</b>	0.488	0.216	<b>0.214</b>	0.222
	MAE	0.379	<b>0.378</b>	0.385	0.362	<b>0.360</b>	0.376	0.243	<b>0.241</b>	0.245	0.280	<b>0.277</b>	0.286	0.194	<b>0.192</b>	0.199	0.378	<b>0.376</b>	0.379	0.110	<b>0.108</b>	0.113	0.820	<b>0.816</b>	0.827	0.399	<b>0.394</b>	0.407	0.286	<b>0.282</b>	0.290
36	MSE	0.327	<b>0.324</b>	0.344	0.344	<b>0.341</b>	0.363	0.172	<b>0.170</b>	0.174	0.255	<b>0.253</b>	0.260	0.120	<b>0.117</b>	0.125	0.305	<b>0.304</b>	0.307	0.037	<b>0.036</b>	0.039	1.583	<b>1.575</b>	1.613	0.637	<b>0.628</b>	0.648	<b>0.288</b>	0.289	0.300
	MAE	0.428	<b>0.427</b>	0.435	0.377	<b>0.375</b>	0.391	0.254	<b>0.252</b>	0.256	0.306	<b>0.303</b>	0.313	0.212	<b>0.210</b>	0.218	0.383	<b>0.381</b>	0.384	0.132	<b>0.130</b>	0.136	0.852	<b>0.848</b>	0.859	0.488	<b>0.481</b>	0.497	<b>0.338</b>	<b>0.338</b>	0.347
48	MSE	0.441	<b>0.438</b>	0.464	0.357	<b>0.354</b>	0.377	0.191	<b>0.189</b>	0.193	0.288	<b>0.284</b>	0.292	0.134	<b>0.131</b>	0.139	0.316	<b>0.315</b>	0.318	0.046	<b>0.045</b>	0.049	1.638	<b>1.630</b>	1.669	0.741	<b>0.731</b>	0.754	<b>0.276</b>	0.280	0.291
	MAE	0.499	<b>0.498</b>	0.507	0.386	<b>0.384</b>	0.401	0.272	<b>0.270</b>	0.274	0.321	<b>0.317</b>	0.327	0.226	<b>0.224</b>	0.232	0.390	<b>0.388</b>	0.391	0.150	<b>0.148</b>	0.154	0.879	<b>0.875</b>	0.886	0.549	<b>0.542</b>	0.560	<b>0.328</b>	0.329	0.338

Table 15. Full result of hyperparameter analysis of the interpolation scheduler. We compare the forecasting performance using linear and cosine schedulers across all benchmark datasets. The best results are in **bold**.

HORIZON METRICS		ENERGY		ETTH1		ETTH2		ETTM1		ETTM2		ENVIRON.		EXCHANGE		HEALTH		WIND		SOLAR	
		Linear	Cosine	Linear	Cosine	Linear	Cosine	Linear	Cosine	Linear	Cosine										
12	MSE	<b>0.140</b>	0.141	<b>0.290</b>	0.293	<b>0.121</b>	0.124	<b>0.140</b>	0.143	<b>0.079</b>	0.084	<b>0.286</b>	<b>0.286</b>	<b>0.015</b>	0.016	<b>1.056</b>	1.060	<b>0.269</b>	0.276	<b>0.115</b>	0.119
	MAE	<b>0.273</b>	0.274	<b>0.343</b>	0.347	<b>0.216</b>	0.219	<b>0.232</b>	0.237	<b>0.167</b>	0.173	<b>0.372</b>	<b>0.370</b>	<b>0.079</b>	0.081	<b>0.697</b>	0.705	<b>0.263</b>	0.266	<b>0.206</b>	0.210
24	MSE	<b>0.265</b>	0.267	<b>0.319</b>	0.322	<b>0.152</b>	0.156	<b>0.213</b>	0.218	<b>0.102</b>	0.108	<b>0.295</b>	<b>0.295</b>	<b>0.026</b>	0.029	<b>1.500</b>	1.506	<b>0.479</b>	0.492	<b>0.216</b>	0.224
	MAE	<b>0.379</b>	0.380	<b>0.362</b>	0.366	<b>0.243</b>	0.247	<b>0.280</b>	0.286	<b>0.194</b>	0.201	<b>0.378</b>	<b>0.376</b>	<b>0.110</b>	0.112	<b>0.820</b>	0.829	<b>0.399</b>	0.403	<b>0.286</b>	0.292
36	MSE	<b>0.327</b>	0.329	<b>0.344</b>	0.348	<b>0.172</b>	0.176	<b>0.255</b>	0.261	<b>0.120</b>	0.127	<b>0.305</b>	<b>0.304</b>	<b>0.037</b>	0.041	<b>1.583</b>	1.589	<b>0.637</b>	0.654	<b>0.288</b>	0.297
	MAE	<b>0.428</b>	0.429	<b>0.377</b>	0.381	<b>0.254</b>	0.258	<b>0.306</b>	0.313	<b>0.212</b>	0.220	<b>0.383</b>	<b>0.381</b>	<b>0.132</b>	0.135	<b>0.852</b>	0.861	<b>0.488</b>	0.493	<b>0.338</b>	0.345
48	MSE	<b>0.441</b>	0.444	<b>0.357</b>	0.361	<b>0.191</b>	0.196	<b>0.288</b>	0.293	<b>0.134</b>	0.142	<b>0.316</b>	<b>0.315</b>	<b>0.046</b>	0.050	<b>1.638</b>	1.645	<b>0.741</b>	0.761	<b>0.276</b>	0.285
	MAE	<b>0.499</b>	0.501	<b>0.386</b>	0.390	<b>0.272</b>	0.276	<b>0.321</b>	0.327	<b>0.226</b>	0.234	<b>0.390</b>	<b>0.388</b>	<b>0.150</b>	0.153	<b>0.879</b>	0.889	<b>0.549</b>	0.554	<b>0.328</b>	0.335

Table 16. Full result of hyperparameter analysis of the patch size. We evaluate the impact of different patch sizes {2, 4, 6, 8, 10} on forecasting performance across all benchmark datasets. The best results are in **bold**.

PATCHSIZE METRICS		2		4		6		8		10	
		MSE	MAE								
Energy	12	0.144	0.278	<b>0.140</b>	<b>0.273</b>	0.147	0.283	0.151	0.289	0.153	0.291
	24	0.272	0.386	<b>0.265</b>	<b>0.379</b>	0.278	0.393	0.286	0.401	0.290	0.404
	36	0.336	0.436	<b>0.327</b>	<b>0.428</b>	0.343	0.443	0.353	0.453	0.358	0.456
	48	0.453	0.508	<b>0.441</b>	<b>0.499</b>	0.463	0.517	0.477	0.528	0.483	0.532
ETTh1	12	0.319	0.370	0.296	0.351	<b>0.290</b>	<b>0.343</b>	0.339	0.389	0.299	0.354
	24	0.362	0.396	0.333	0.375	<b>0.319</b>	<b>0.362</b>	0.385	0.417	0.340	0.379
	36	0.400	0.417	0.365	0.394	<b>0.344</b>	<b>0.377</b>	0.425	0.439	0.375	0.399
	48	0.420	0.429	0.382	0.404	<b>0.357</b>	<b>0.386</b>	0.447	0.451	0.394	0.410
ETTh2	12	0.157	0.242	<b>0.121</b>	<b>0.216</b>	0.140	0.234	0.137	0.228	0.140	0.222
	24	0.197	0.273	<b>0.152</b>	<b>0.243</b>	0.175	0.263	0.171	0.256	0.175	0.249
	36	0.222	0.285	<b>0.172</b>	<b>0.254</b>	0.198	0.275	0.194	0.268	0.198	0.261
	48	0.246	0.305	<b>0.191</b>	<b>0.272</b>	0.220	0.294	0.215	0.287	0.220	0.279
ETTm1	12	0.144	0.238	<b>0.140</b>	<b>0.232</b>	0.154	0.245	0.155	0.246	0.152	0.244
	24	0.220	0.287	<b>0.213</b>	<b>0.280</b>	0.234	0.296	0.236	0.297	0.231	0.294
	36	0.263	0.314	<b>0.255</b>	<b>0.306</b>	0.280	0.323	0.282	0.325	0.277	0.321
	48	0.297	0.329	<b>0.288</b>	<b>0.321</b>	0.316	0.339	0.319	0.340	0.312	0.337
ETTm2	12	0.097	0.188	0.094	0.185	<b>0.079</b>	<b>0.167</b>	0.081	0.171	0.093	0.183
	24	0.126	0.219	0.122	0.215	<b>0.102</b>	<b>0.194</b>	0.105	0.198	0.121	0.213
	36	0.148	0.239	0.143	0.235	<b>0.120</b>	<b>0.212</b>	0.124	0.217	0.142	0.233
	48	0.165	0.255	0.160	0.250	<b>0.134</b>	<b>0.226</b>	0.138	0.231	0.158	0.248
Environ.	12	<b>0.286</b>	<b>0.372</b>	0.305	0.397	0.315	0.408	0.315	0.409	0.441	0.481
	24	<b>0.295</b>	<b>0.378</b>	0.316	0.406	0.330	0.417	0.332	0.421	0.437	0.481
	36	<b>0.305</b>	<b>0.383</b>	0.331	0.416	0.346	0.427	0.355	0.436	0.445	0.485
	48	<b>0.316</b>	<b>0.390</b>	0.343	0.425	0.363	0.438	0.379	0.453	0.451	0.488
Exchange	12	<b>0.015</b>	0.081	<b>0.015</b>	<b>0.079</b>	<b>0.015</b>	0.080	<b>0.015</b>	<b>0.079</b>	<b>0.015</b>	0.080
	24	0.028	0.113	<b>0.026</b>	0.110	<b>0.026</b>	<b>0.109</b>	<b>0.026</b>	<b>0.109</b>	<b>0.026</b>	<b>0.109</b>
	36	0.040	0.137	<b>0.037</b>	0.132	<b>0.037</b>	<b>0.131</b>	<b>0.037</b>	0.132	<b>0.037</b>	<b>0.131</b>
	48	0.053	0.158	<b>0.046</b>	<b>0.150</b>	0.048	<b>0.150</b>	0.049	0.153	0.048	<b>0.150</b>
Health	12	1.759	0.940	1.327	0.788	<b>1.056</b>	<b>0.697</b>	2.966	1.298	2.831	1.258
	24	1.984	1.011	1.750	0.909	<b>1.500</b>	<b>0.820</b>	2.946	1.290	2.755	1.245
	36	2.058	1.021	1.757	0.918	<b>1.583</b>	<b>0.852</b>	2.900	1.270	2.755	1.229
	48	2.126	1.052	1.912	0.965	<b>1.638</b>	<b>0.879</b>	2.974	1.278	2.788	1.235
Wind	12	0.298	0.295	<b>0.269</b>	<b>0.263</b>	0.277	0.271	0.289	0.287	0.302	0.299
	24	0.530	0.448	<b>0.479</b>	<b>0.399</b>	0.493	0.411	0.515	0.435	0.537	0.454
	36	0.705	0.548	<b>0.637</b>	<b>0.488</b>	0.656	0.502	0.684	0.532	0.714	0.555
	48	0.820	0.617	<b>0.741</b>	<b>0.549</b>	0.763	0.565	0.796	0.598	0.831	0.624
Solar	12	0.122	0.215	<b>0.115</b>	<b>0.206</b>	0.121	0.213	0.124	0.217	0.130	0.225
	24	0.230	0.298	<b>0.216</b>	<b>0.285</b>	0.228	0.295	0.233	0.301	0.244	0.311
	36	0.311	0.358	<b>0.288</b>	<b>0.338</b>	0.309	0.354	0.315	0.361	0.331	0.374
	48	0.302	0.349	<b>0.276</b>	<b>0.328</b>	0.300	0.345	0.306	0.352	0.322	0.365

Table 17. Full results of the comparative analysis on backbone architectures. We evaluate the performance of the vanilla transformer against Qwen LLM family with varying parameter scales (0.6B, 1.7B, and 4B) across all benchmark datasets. The best results are in **bold**.

BACKBONE METRICS		TRANSFORMER		QWEN3-0.6B		QWEN3-1.7B		QWEN3-4B	
		MSE	MAE	MSE	MAE	MSE	MAE	MSE	MAE
Energy	12	0.144	0.276	0.140	0.273	0.141	0.274	<b>0.138</b>	<b>0.271</b>
	24	0.272	0.383	0.265	0.379	0.267	0.380	<b>0.262</b>	<b>0.376</b>
	36	0.336	0.433	0.327	0.428	0.329	0.429	<b>0.323</b>	<b>0.425</b>
	48	0.453	0.504	0.441	0.499	0.444	0.501	<b>0.436</b>	<b>0.495</b>
ETTh1	12	0.305	0.356	0.290	0.343	0.290	0.341	<b>0.286</b>	<b>0.339</b>
	24	0.335	0.376	0.319	0.362	0.319	0.360	<b>0.315</b>	<b>0.358</b>
	36	0.361	0.391	0.344	0.377	0.344	0.375	<b>0.339</b>	<b>0.373</b>
	48	0.375	0.401	0.357	0.386	0.356	0.384	<b>0.352</b>	<b>0.382</b>
ETTh2	12	0.131	0.226	0.121	0.216	0.122	0.217	<b>0.118</b>	<b>0.211</b>
	24	0.164	0.255	0.152	0.243	0.153	0.244	<b>0.148</b>	<b>0.238</b>
	36	0.186	0.266	0.172	0.254	0.173	0.255	<b>0.168</b>	<b>0.249</b>
	48	0.206	0.285	0.191	0.272	0.192	0.273	<b>0.186</b>	<b>0.266</b>
ETTm1	12	0.151	0.242	0.140	0.232	0.139	0.231	<b>0.137</b>	<b>0.229</b>
	24	0.229	0.292	0.213	0.280	0.212	0.279	<b>0.208</b>	<b>0.276</b>
	36	0.274	0.319	0.255	0.306	0.254	0.305	<b>0.249</b>	<b>0.302</b>
	48	0.309	0.334	0.288	0.320	0.286	0.319	<b>0.281</b>	<b>0.316</b>
ETTm2	12	0.092	0.182	0.079	0.167	0.079	0.169	<b>0.076</b>	<b>0.165</b>
	24	0.118	0.212	0.102	0.194	0.102	0.196	<b>0.098</b>	<b>0.191</b>
	36	0.139	0.231	0.120	0.212	0.120	0.214	<b>0.115</b>	<b>0.209</b>
	48	0.155	0.247	0.134	0.226	0.134	0.229	<b>0.128</b>	<b>0.223</b>
Environ.	12	0.296	<b>0.279</b>	0.286	0.372	0.285	0.371	<b>0.283</b>	0.367
	24	0.305	0.385	0.295	0.378	0.294	0.377	<b>0.292</b>	<b>0.373</b>
	36	0.316	0.390	0.305	0.383	0.304	0.382	<b>0.301</b>	<b>0.378</b>
	48	0.327	0.397	0.316	0.390	0.316	0.389	<b>0.312</b>	<b>0.385</b>
Exchange	12	0.018	0.083	0.015	0.079	0.015	0.079	<b>0.014</b>	<b>0.077</b>
	24	0.031	0.115	0.026	0.110	0.026	0.109	<b>0.024</b>	<b>0.107</b>
	36	0.044	0.138	0.037	0.132	0.037	0.131	<b>0.035</b>	<b>0.129</b>
	48	0.055	0.157	0.046	0.150	0.046	0.149	<b>0.043</b>	<b>0.146</b>
Health	12	1.105	0.706	1.056	0.697	1.056	0.696	<b>1.052</b>	<b>0.694</b>
	24	1.570	0.831	1.500	0.820	1.500	0.819	<b>1.494</b>	<b>0.816</b>
	36	1.657	0.863	1.583	0.852	1.583	0.851	<b>1.577</b>	<b>0.848</b>
	48	1.715	0.891	1.638	0.879	1.638	0.878	<b>1.632</b>	<b>0.875</b>
Wind	12	0.297	0.285	0.269	0.263	0.268	0.263	<b>0.266</b>	<b>0.258</b>
	24	0.529	0.433	0.479	0.399	0.478	0.398	<b>0.473</b>	<b>0.392</b>
	36	0.704	0.530	0.637	0.488	0.635	0.487	<b>0.629</b>	<b>0.479</b>
	48	0.818	0.596	0.741	0.549	0.739	0.548	<b>0.732</b>	<b>0.539</b>
Solar	12	0.137	0.222	0.115	0.206	0.116	0.206	<b>0.114</b>	<b>0.203</b>
	24	0.258	0.308	0.216	0.286	0.218	0.286	<b>0.214</b>	<b>0.282</b>
	36	0.347	0.370	<b>0.288</b>	<b>0.338</b>	0.295	0.343	0.289	<b>0.338</b>
	48	0.338	0.360	<b>0.276</b>	<b>0.328</b>	0.285	0.333	0.280	<b>0.328</b>

Table 18. Full results of the analysis on the look-back window length. We evaluate the impact of extended look-back window length  $L \in \{96, 192, 336\}$  on forecasting performance across all benchmark datasets. The best results are in **bold**.

HORIZON METRICS	ENERGY			ETTh1			ETTh2			ETTM1			ETTM2			ENVIRON.			EXCHANGE			HEALTH			WIND			SOLAR			
	96	192	336	96	192	336	96	192	336	96	192	336	96	192	336	96	192	336	96	192	336	96	192	336	96	192	336				
12	MSE	0.140	0.138	<b>0.137</b>	0.290	0.289	<b>0.284</b>	0.121	0.120	<b>0.118</b>	0.140	0.139	<b>0.137</b>	0.079	0.078	<b>0.077</b>	0.286	0.285	<b>0.266</b>	0.015	0.015	<b>0.014</b>	1.056	1.052	<b>1.044</b>	0.269	0.267	<b>0.260</b>	0.115	0.115	<b>0.113</b>
	MAE	0.273	0.272	<b>0.270</b>	0.343	0.342	<b>0.338</b>	0.216	0.214	<b>0.211</b>	0.232	0.231	<b>0.229</b>	0.167	0.168	<b>0.166</b>	0.372	0.371	<b>0.266</b>	0.079	0.081	<b>0.077</b>	0.697	0.695	<b>0.691</b>	0.263	0.261	<b>0.256</b>	0.206	0.207	<b>0.202</b>
24	MSE	0.265	0.262	<b>0.260</b>	0.319	0.318	<b>0.313</b>	0.152	0.151	<b>0.148</b>	0.213	0.212	<b>0.208</b>	0.102	0.101	<b>0.099</b>	0.295	0.294	<b>0.275</b>	0.026	0.027	<b>0.024</b>	1.500	1.495	<b>1.483</b>	0.479	0.475	<b>0.463</b>	0.216	0.216	<b>0.213</b>
	MAE	0.379	0.377	<b>0.374</b>	0.362	0.361	<b>0.357</b>	0.243	0.241	<b>0.238</b>	0.280	0.279	<b>0.276</b>	0.194	0.195	<b>0.192</b>	0.378	0.377	<b>0.372</b>	0.110	0.112	<b>0.107</b>	0.820	0.818	<b>0.813</b>	0.399	0.395	<b>0.388</b>	0.286	0.287	<b>0.281</b>
36	MSE	0.327	0.323	<b>0.321</b>	0.344	0.342	<b>0.337</b>	0.172	0.171	<b>0.168</b>	0.255	0.254	<b>0.249</b>	0.120	0.119	<b>0.117</b>	0.305	0.303	<b>0.284</b>	0.037	0.038	<b>0.035</b>	1.583	1.577	<b>1.565</b>	0.637	0.632	<b>0.616</b>	<b>0.288</b>	0.292	<b>0.288</b>
	MAE	0.428	0.426	<b>0.423</b>	0.377	0.376	<b>0.372</b>	0.254	0.252	<b>0.249</b>	0.306	0.305	<b>0.302</b>	0.212	0.213	<b>0.210</b>	0.383	0.382	<b>0.377</b>	0.132	0.135	<b>0.129</b>	0.852	0.850	<b>0.845</b>	0.488	0.484	<b>0.475</b>	0.338	0.344	<b>0.337</b>
48	MSE	0.441	0.436	<b>0.433</b>	0.357	0.355	<b>0.350</b>	0.191	0.190	<b>0.186</b>	0.288	0.286	<b>0.281</b>	0.134	0.133	<b>0.131</b>	0.316	0.314	<b>0.294</b>	0.046	0.047	<b>0.043</b>	1.638	1.632	<b>1.620</b>	0.741	0.735	<b>0.717</b>	<b>0.276</b>	0.283	<b>0.279</b>
	MAE	0.499	0.497	<b>0.493</b>	0.386	0.385	<b>0.381</b>	0.272	0.270	<b>0.266</b>	0.321	0.319	<b>0.316</b>	0.226	0.227	<b>0.224</b>	0.390	0.389	<b>0.384</b>	0.150	0.153	<b>0.146</b>	0.879	0.877	<b>0.871</b>	0.549	0.544	<b>0.534</b>	<b>0.328</b>	0.335	<b>0.328</b>